competent adenovirus OBP-401, which induces ectopic GFP expression in tumor cells, but not in normal cells.[32] OBP-401 infection efficiently induces GFP expression in metastatic tumor cells at regional lymph nodes[32] and liver,[33] circulating tumor cells in blood flow[34] and disseminated tumor cells in the abdominal cavity.[35] These results suggest that OBP-401 is a highly sensitive tool for the detection of tumor cells. Furthermore, Ad5-based OBP-401 would also be useful for induction of GFP expression in CAR-positive tumor cells, but not in CAR-negative tumor cells.

In the present study, we evaluated whether induction of GFP expression by OBP-401 infection is associated with CAR expression in tumor cells. OBP-401-mediated GFP induction was further examined in xenograft tumor tissues that have different levels of CAR expression and in surrounding normal tissues.

RESULTS AND DISCUSSION

Assessment of an OBP-401 infection protocol for the detection of CAR-positive tumor cells

We recently demonstrated that the level of CAR expression that was detected using flow cytometry was significantly associated with OBP-301-mediated cytopathic activity in human bone and soft tissue sarcoma cells.[29] Furthermore, OBP-401 infection has been shown to induce GFP expression 24 h after infection of human sarcoma cells.[34] To evaluate whether GFP expression that is induced by OBP-401 infection is associated with CAR expression in tumor cells, we used three human sarcoma cell lines (OST, NMFH-1 and OUMS-27) that have different levels of CAR expression, as previously reported.[29] Flow cytometric analysis confirmed that OST cells showed detectable CAR expression, whereas cells of the NMFH-1 and OUMS-27 sarcoma cell lines had no detectable CAR expression (Figure 1a).

To determine suitable conditions for OBP-401 infection in order to detect CAR-positive tumor cells, OST sarcoma cells were infected with OBP-401 at multiplicity of infections (MOIs) of 1, 10 and 100 plaque-forming units (PFU) per cell over 24 h (Figure 1b and c). Twelve hours after infection, only OBP-401 infection at an MOI of 100 had induced GFP expression in all of the OST cells. Twenty-four hours after infection, OBP-401 infection at MOIs of 10 and 100 had induced ectopic GFP expression in all of the OST cells, whereas OBP-401 infection at an MOI of 1 had induced GFP expression in about 80% of the OST cells. These results indicate that OBP-401 infection at an MOI of greater than 10 is necessary to efficiently detect CAR-positive tumor cells 24 h after infection.

To subsequently determine a suitable condition for OBP-401 infection that would exclude CAR-negative tumor cells, the NMFH-1 and OUMS-27 sarcoma cells that do not express CAR were infected with OBP-401 at MOIs of 10 and 100 for 60 h (Figures 1d and e). NMFH-1 cells expressed GFP at 24 and 48 h after OBP-401 infection at MOIs of 100 and 10, respectively. In contrast, OUMS-27 cells exhibited no GFP expression after OBP-401 infection. To investigate the different GFP expression between these CAR-negative tumor cells, expression of integrins, $\alpha v\beta 3$ and $\alpha v\beta 5$, was further examined by flow cytometry. NMFH-1 cells showed twofold higher expression of integrin $\alpha v\beta 3$ compared with OUMS-27 cells, whereas $\alpha v\beta 5$ expression was similar in these cells (Supplementary Figure S1a). These results indicate that OBP-401 infection at an MOI of 10 for 24 h is a suitable protocol for distinguishing CAR-negative tumor cells from CAR-positive tumor cells, when CAR-negative tumor cells express integrin molecules.

Relationship between OBP-401-induced GFP expression and CAR expression

To evaluate whether OBP-401-induced GFP expression correlates with CAR expression in tumor cells, six human sarcoma cell lines (OST, U2OS, NOS-10, MNNG/HOS, NMFH-1 and OUMS-27) and normal human lung fibroblasts (NHLF) cells that have different levels of CAR expression (Figure 1a and Supplementary Figure S1b) were infected with OBP-401 at an MOI of 10 for 24 h, and the GFP-positive cells in each cell type were analyzed under fluorescence microscopy (Figures 2a and b). OBP-401 infection-induced GFP expression from 12 h after infection and, after 24 h, more than 40% of all CAR-positive tumor cells (OST, U2OS, NOS-10 and MNNG/HOS) were detected as GFP-positive cells. However, no GFP-positive cells were detected in the CAR-negative tumor cells (NMFH-1, OUMS-27), or in the normal NHLF cells, 24 h after infection. Furthermore, OBP-401-mediated GFP induction in CAR-positive tumor cells was suppressed by blocking CAR proteins with anti-CAR antibody (Supplementary Figure S2). To assess the GFP expression level in all tumor and normal cells in a more quantitative manner, we quantified the level of GFP fluorescence in each cell type 24 h after infection using a fluorescence microplate reader (Figure 2c). We also quantified the level of CAR expression in these cells by calculating the mean fluorescence intensity in flow cytometric analysis (Figure 2d). GFP fluorescence was detected in CAR-positive tumor cells, but not in either CAR-negative tumor cells or in CAR-positive normal cells. There was a significant relationship between the CAR expression level and the GFP fluorescence level ($r = 0.885$; $P = 0.019$) (Figure 2e). These results indicate that OBP-401-mediated GFP expression is highly associated with CAR expression in tumor cells.

Comparison of the potential of OBP-401-mediated GFP induction and of conventional methods for CAR detection

To estimate the potential of OBP-401-mediated GFP induction for the detection of CAR-positive tumor cells, we compared the above protocol using OBP-401 with western blot analysis and immunocytochemistry. CAR expression was detected in OST, U2OS and NOS-10 sarcoma cells, but not in CAR-positive MNNG/HOS sarcoma cells, using western blot analysis (Supplementary Figure S3a). In contrast, only OST cells displayed a positive CAR signal using immunocytochemistry, whereas the CAR signal of the other three CAR-positive tumor cells was almost as weak as that from CAR-negative tumor cells (Supplementary Figure S3b). CAR expression was also not detected in CAR-positive NHLF cells by either western blot analysis or by immunocytochemistry. These results suggest that the GFP induction protocol using OBP-401 is more sensitive for the detection of CAR-positive tumor cells than conventional methods.

OBP-401-mediated GFP induction was detected in MNNG/HOS sarcoma cells that expressed a low level of CAR (Figure 2c), although neither western blot analysis nor immunocytochemistry detected CAR in these cells (Supplementary Figure S3). Furthermore, although conventional methods may be able to detect high CAR expression in tumor cells, whether the CAR expression that is detected by conventional methods is really functional for binding with Ad5-based vectors still remains unclear. In contrast, as OBP-401 is an Ad5-based vector that expresses a fluorescent *GFP* gene, OBP-401-induced GFP expression directly proves that the CAR that is expressed is functional for Ad5-based vector binding. Thus, the OBP-401-mediated GFP induction strategy is a potential diagnostic method that can efficiently and directly assess functional CAR expression in tumor cells.

OBP-401-mediated GFP induction in xenograft tumor and normal tissues with different CAR expression

Finally, to investigate the potential of the OBP-401-mediated method for the detection of CAR expression in tumor and normal tissues, we used this method to analyze CAR expression of human xenograft tumor tissues, that do or do not express CAR, as well as of surrounding normal muscle tissues, which have been previously shown to lose CAR expression.[36] CAR-positive OST sarcoma cells or CAR-negative OUMS-27 sarcoma cells were inoculated into nude

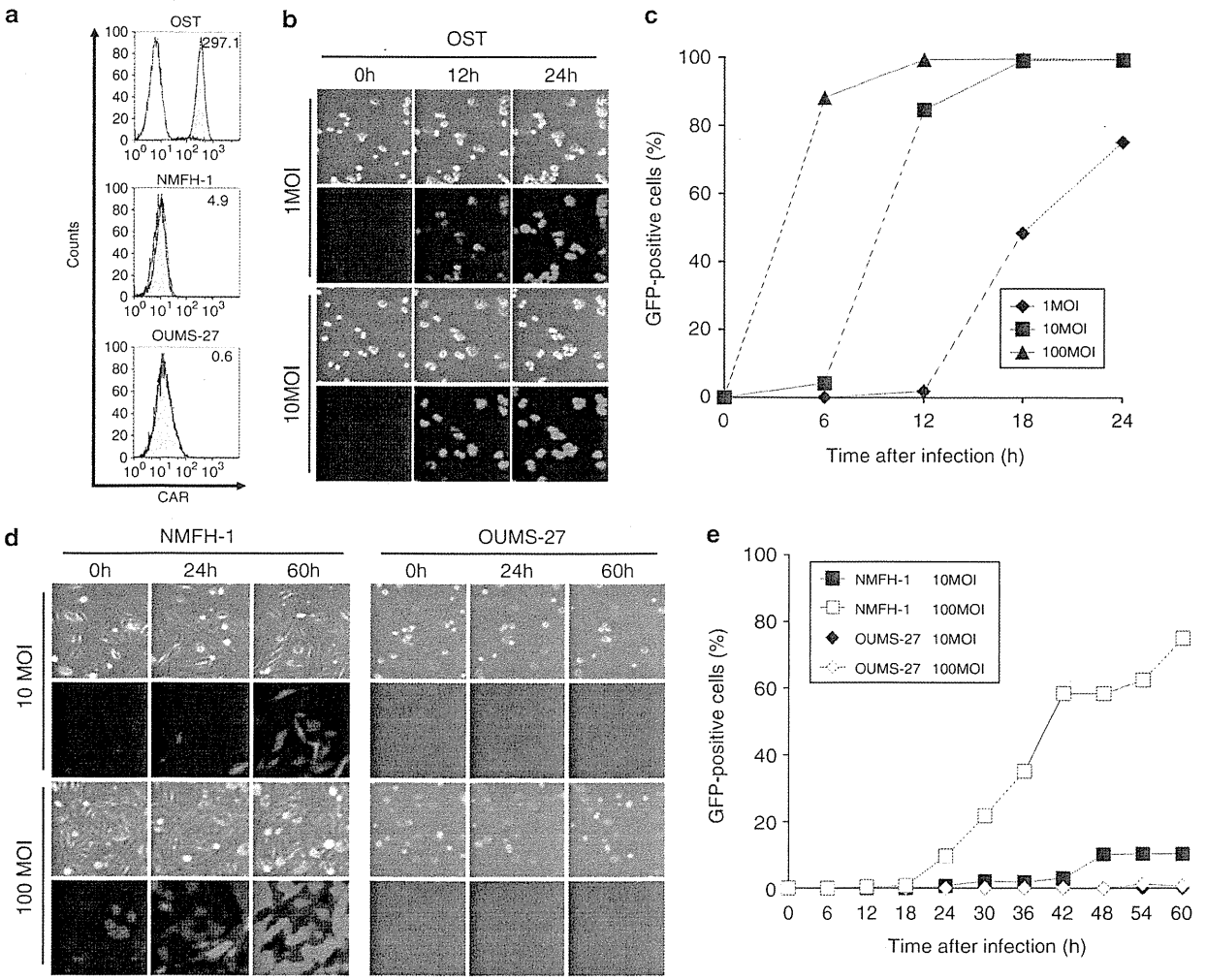

Figure 1. Establishment of a suitable protocol for the detection of CAR expression using OBP-401. (**a**) The level of CAR expression on three human sarcoma cell lines (OST, NMFH-1 and OUMS-27) was analyzed using flow cytometry. The cells were incubated with a monoclonal anti-CAR (RmcB) antibody and the signal was detected using a fluorescent isothiocyanate (FITC)-labeled secondary antibody. The mean fluorescence intensity (MFI), which is a measure of CAR and integrin expression, was calculated for each cell and is shown at the top right of each graph. (**b**) Time-lapse images of OST cells, which displayed the highest CAR expression, were recorded for 24 h after OBP-401 infection at MOIs of 1 and 10 PFU per cell. Representative images taken at the indicated time points and MOIs show cell morphology that was analyzed using phase-contrast microscopy (top panels) and GFP expression that was analyzed using fluorescence microscopy (bottom panels). Original magnification: × 80. (**c**) The percentage of GFP-positive cells was counted in OST cells at the indicated time points after OBP-301 infection at MOIs of 1, 10 and 100 PFU per cell. (**d**) Time-lapse images of non-CAR-expressing OUMS-27 and NMFH-1 cells were recorded for 60 h after OBP-401 infection at MOIs of 10 and 100 PFU per cell. Representative images taken at the indicated time points and MOIs show cell morphology that was analyzed using phase-contrast microscopy (top panels) and GFP expression that was analyzed using fluorescence microscopy (bottom panels). Original magnification: × 80. (**e**) The percentage of OUMS-27 and NMFH-1 GFP-positive cells was counted at the indicated time points after OBP-301 infection at MOIs of 10 and 100 PFU per cell.

mice to develop xenograft tumors. After resection of the OST tumors, the OUMS-27 tumors and normal muscle tissue, the tissues were subjected to the protocol for OBP-401-mediated GFP induction using a three-step procedure (Figure 3a) as follows; step 1: OBP-401 infection for 24 h, step 2: washing with PBS and step 3: observation under a fluorescence microscope. As shown in Figure 3b, OBP-401 infection-induced GFP expression in CAR-positive OST tumor tissues, but not in CAR-negative OUMS-27 tumor tissues or in normal muscle tissue. These results suggest that OBP-401-mediated GFP induction is a simple and useful method for the detection of CAR expression by tumor tissues.

Flow cytometry is a highly sensitive conventional method for the detection of cell surface CAR expression, which is associated with the therapeutic efficacy of Ad5-based vectors in tumor cells.[13,24,28,29] However, as many tumor cells tightly bind to each other or to normal stromal cells within tumor tissues, the preparation of single tumor cells is not easy, and therefore flow cytometry is an inadequate method for the detection of CAR expression in tumor tissues. In contrast, the preparation of single tumor cells is not necessary for the OBP-401-mediated GFP induction protocol. Furthermore, assay of OBP-401-induced GFP expression was more sensitive than flow cytometry (Figure 2d) in distinguishing CAR-positive normal cells from CAR-positive tumor cells (Figure 2c). Thus, the OBP-401-mediated GFP induction method is a simple and tumor-specific system for the detection of CAR expression in tumor tissues.

Fluorescent proteins including GFP have great potentials to visualize tumor cells in real time on the *in vivo* setting.[37,38]

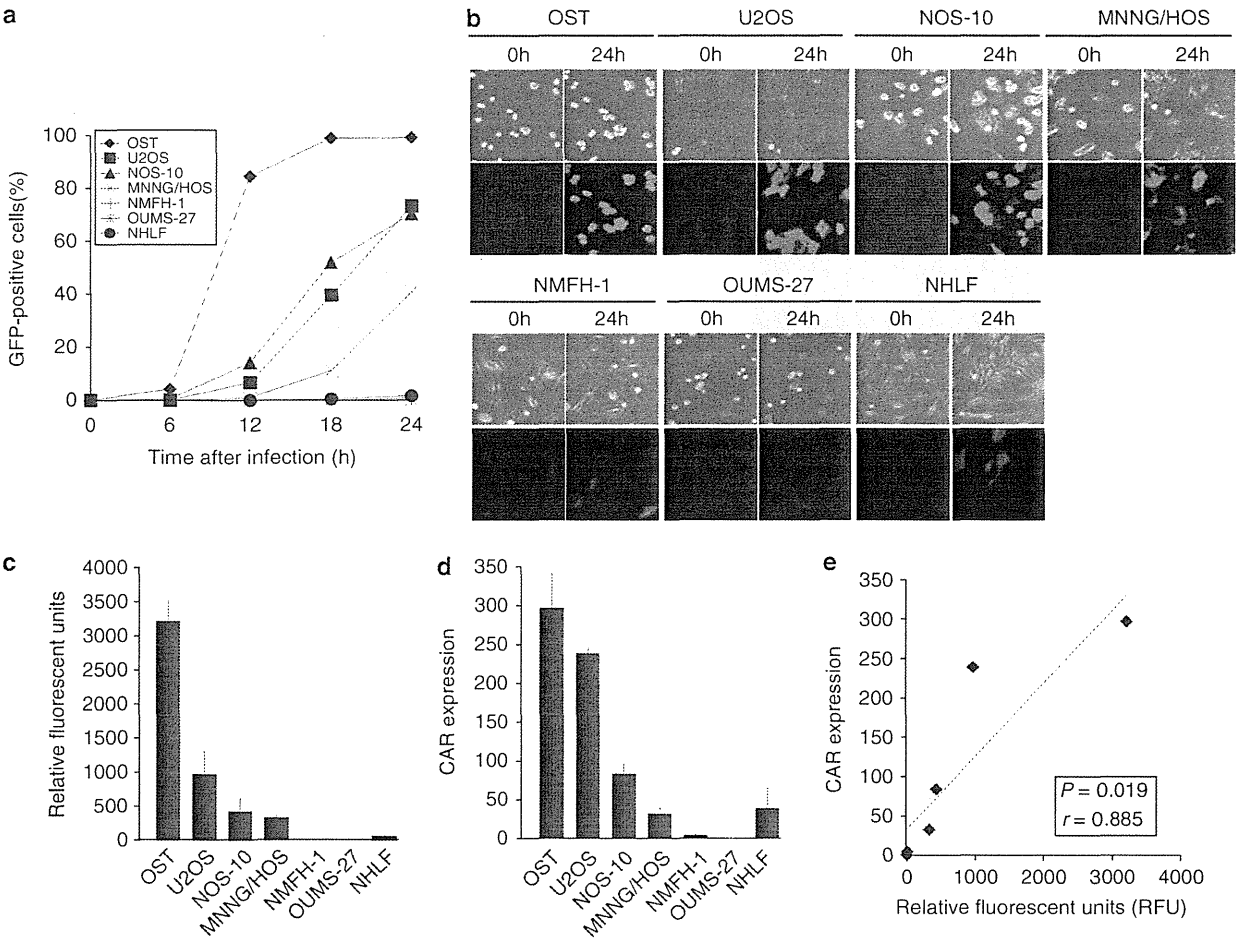

Figure 2. *In vitro* CAR-dependent GFP expression induced by OBP-401 infection. (**a**) The percentage of GFP-positive cells in all tumor and normal cells was counted at the indicated time points after OBP-301 infection at an MOI of 10 PFU per cell. (**b**) Time-lapse images of all tumor and normal cells were recorded for 24 h after infection with OBP-401 at an MOI of 10 PFU per cell. Representative images taken at the indicated time points show cell morphology that was analyzed using phase-contrast microscopy (top panels) and GFP expression that was analyzed using fluorescence microscopy (bottom panels). Original magnification: ×80. (**c**) Quantitative assessment of the level of GFP fluorescence in all tumor and normal cells 24 after OBP-401 infection at an MOI of 10 PFU per cell, using a fluorescent microplate reader with excitation/emission at 485 nm/528 nm. The intensity of GFP fluorescence was evaluated based on the brightness determinations used as relative fluorescence units (RFU). (**d**) The mean fluorescent intensity (MFI) of (CAR) expression on human sarcoma cells and normal fibroblasts. The cells were incubated with a monoclonal anti-CAR (RmcB) antibody, followed by a FITC-labeled secondary antibody, and were analyzed using flow cytometry. (**e**) Relationship between the level of GFP fluorescence and CAR expression in all tumor and normal cells after OBP-401 infection. The slope represents the inverse correlation between these two factors. Statistical significance was determined as $P<0.05$, after analysis of Pearson's correlation coefficient.

We previously reported that OBP-401 can efficiently induce GFP expression in small populations of metastatic tumor cells at various regions *in vivo*.[32–35] In this study, we further demonstrated that OBP-401-mediated GFP expression provides us the important information for detection of CAR-positive tumor cells. OBP-401 with *hTERT* gene promoter-induced GFP expression in CAR-positive tumor cells with telomerase activity, but not CAR-positive normal cells without telomerase activity (Figure 2c). There was significant relationship between the CAR expression and the GFP expression in tumor cells (Figure 2d). Among the four CAR-positive tumor cells, U2OS cells showed low GFP expression compared with high CAR expression (Figure 1a and 2c). As we recently reported that U2OS cells showed low *hTERT* mRNA expression, the low activity of *hTERT* gene promoter in tumor cells would affect OBP-401-mediated GFP expression. However, as various types of human cancer cells frequently show high telomerase activities,[39] OBP-401-mediated GFP induction system would be widely useful method to evaluate CAR expression in tumor cells.

Previous reports have suggested that *ex vivo* infection of human cancer specimens with a GFP-expressing replication-deficient adenovirus[40] or a replication-selective oncolytic adenovirus[41] is a useful method for assessment of the transduction efficacy or cytopathic activity, respectively, of Ad5-based vectors in individual tumor tissues. In this study, we confirmed that the GFP-expressing telomerase-specific oncolytic adenovirus OBP-401 is useful for detection of CAR-positive tumor tissues through induction of GFP expression (Figure 3b). Interestingly, OBP-401-infected OST tumor tissues showed heterogenous GFP expression (Figure 3b), although GFP expression was induced in all OBP-401-infected OST cells *in vitro* (Figure 2b). Our finding of heterogenous GFP expression in tumor tissues, which indicates heterogenous CAR expression, is consistent with a previously reported heterogeneity in CAR expression.[42] As several factors such as hypoxia[43] and cell cycle status[44] have been suggested to affect CAR expression in tumor cells, factors in the tumor microenvironment may be involved in the heterogenous CAR expression in tumor cells.

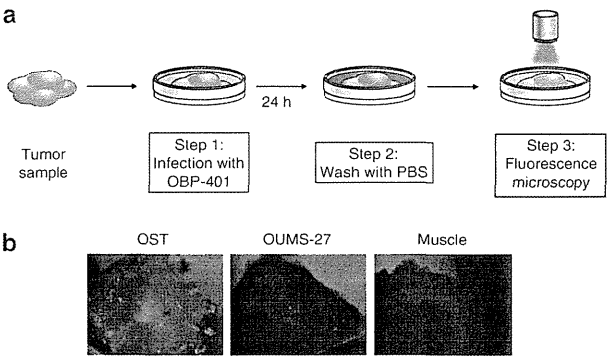

Figure 3. A simple method for detection of CAR expression in tumor tissues using OBP-401 infection. (**a**) Outline of the 3-step procedure; step 1: infection with OBP-401, step 2: washing with PBS and step 3: observation under a fluorescence microscope. Tumor tissues ($2 \times 2 \times 2\,mm^3$) were infected with OBP-401 at a concentration of 2.4×10^6 PFU for 24 h, were washed with PBS and were observed using fluorescence microscopy. (**b**) Assessment of GFP expression in the CAR-positive OST tumor (left panel), the CAR-negative OUMS-27 tumor (middle panel) and normal muscle tissues (right panel) under a fluorescence microscope. Original magnification: × 30.

Furthermore, as OBP-401 induces tumor-specific GFP expression, normal stromal or epithelial cells may be involved in heterogenous GFP expression in tumor tissues.

In conclusion, we have demonstrated that the GFP-expressing telomerase-specific replication-competent adenovirus OBP-401 is a promising fluorescence imaging tool for the detection of functional and tumor-specific CAR expression in tumor tissues. OBP-401-mediated GFP induction is a simple and highly sensitive method for analysis of tumor cells compared with conventional methods. This novel CAR detection system using OBP-401 has the potential of being widely applicable to assessment of predictive biomarkers for Ad5-based vector-mediated anticancer therapy.

MATERIALS AND METHODS

Cell lines

The human osteosarcoma cell line OST was kindly provided by Dr Satoru Kyo (Kanazawa University, Ishikawa, Japan). The human osteosarcoma cell line U2OS and the transformed embryonic kidney cell line 293 were obtained from the American Type Culture Collection (ATCC; Manassas, VA, USA). The human osteosarcoma cell line NOS-10[45] and the human malignant fibrous histiocytoma cell line NMFH-1[46] were kindly provided by Dr Hiroyuki Kawashima (Niigata University, Niigata, Japan). The human osteosarcoma cell line MNNG/HOS was purchased from DS Pharma Biomedical (Osaka, Japan). The chondrosarcoma cell line OUMS-27 was previously established in our laboratory.[47] The normal human lung fibroblast cell line NHLF was obtained from TaKaRa Biomedicals (Kyoto, Japan). These cells were propagated as monolayer cultures in the medium recommended by the manufacturer. All media were supplemented with 10% heat-inactivated fetal bovine serum, 100 units ml^{-1} penicillin and 100 μg ml^{-1} streptomycin. The cells were maintained at 37 °C in a humidified atmosphere containing 5% CO_2.

Recombinant adenoviruses

We previously generated and characterized OBP-401, which is a telomerase-specific replication-competent adenovirus variant, in which the *hTERT* promoter element drives the expression of *E1A* and *E1B* genes that are linked to an internal ribosome entry site, and in which the *GFP* gene is inserted into the E3 region under a cytomegalovirus promoter.[32,34] The virus was purified by ultracentrifugation using cesium chloride step gradients. Viral titers were determined by a plaque-forming assay using 293 cells and viruses were stored at −80 °C.

Flow cytometry

The cells (5×10^5 cells) were labeled with the mouse monoclonal anti-CAR (RmcB; Upstate Biotechnology, Lake Placid, NY, USA) antibody for 30 min at 4 °C. The cells were then incubated with fluorescent isothiocyanate-conjugated rabbit anti-mouse IgG second antibody (Zymed Laboratories, San Francisco, CA, USA) and were analyzed using flow cytometry (FACS Array; Becton Dickinson, Mountain View, CA, USA). The mean fluorescence intensity of CAR for each cell line was determined by calculating the differences between the mean fluorescence intensity in antibody-treated and non-treated cells in triplicate experiments.

Time-lapse confocal laser microscopy

The cells (1×10^5 cells per dish) were seeded in 35 mm glass-based dishes 20 h before virus infection. OST cells were infected with OBP-401 at an MOI of 1, 10 or 100 PFU per cell for 24 h. NMFH-1 and OUMS-27 cells were infected with OBP-401 at an MOI of 10 or 100 PFU per cell for 60 h. Other cells were infected with OBP-401 at an MOI of 10 PFU per cell for 24 h. Phase-contrast and fluorescence time-lapse recordings were obtained to concomitantly analyze cell morphology and GFP expression using an inverted FV10i confocal laser scanning microscopy (OLYMPUS; Tokyo, Japan). Photographic images were taken every 5 min. The percentage of GFP-positive cells in each field was calculated using the formula: the number of CAR-positive cells / the total number of CAR-positive and CAR-negative cells × 100.

Fluorescence microplate assay

The cells (5×10^3 cells per well) were seeded on 96-well black bottomed culture plates and were incubated for 20 h before virus infection. The cells were infected with OBP-401 at an MOI of 10 for 24 h. The level of expression of GFP fluorescence was measured using a fluorescent microplate reader (DS Pharma Biomedical; Osaka, Japan) with excitation/emission at 485 nm/528 nm. The mean expression of GFP fluorescence in each cell was calculated in triplicate experiments, as previously reported.[34]

Animal experiments

Animal experimental protocols were approved by the Ethics Review Committee for Animal Experimentation of Okayama University School of Medicine. OST and OUMS-27 cells (5×10^6 cells per site) were inoculated into the flank of female athymic nude mice aged 6 to 7 weeks (Charles River Laboratories, Wilmington, MA, USA). Palpable tumors developed within 14 to 21 days and were permitted to grow to ~5 to 6 mm in diameter. At that stage, tumor and normal muscle tissues were resected. The tumor and normal tissues ($2 \times 2 \times 2\,mm^3$) were placed in 96-well plates with culture medium. As single tumor cell is about 10 μm in diameter, we considered that there are 2.4×10^5 cells on the surface area of each sample tissue. Then, we infected each sample tissue with 2.4×10^6 PFU (10 MOI per sample) of OBP-401 for 24 h. After washing with PBS, tumor and normal tissues were again placed in 96-well plates with culture medium and analyzed using an inverted fluorescence microscope (OLYMPUS).

Statistical analysis

Data are expressed as means ± s.d. Student's *t*-test was used to compare differences between groups. Pearson's product-moment correlation coefficients were calculated using PASW statistics software version 18 (SPSS Inc., Chicago, IL, USA). Statistical significance was defined as when the *P* value was less than 0.05.

ABBREVIATIONS

Ad5, Adenovirus serotype 5; CAR, coxsackie and adenovirus receptor; GFP, green fluorescent protein; RT-PCR, reverse transcription-polymerase chain reaction; hTERT, human telomerase reverse transcriptase; MOI, multiplicity of infection;

PFU, plaque-forming unit; IRES, internal ribosome entry site; FITC, fluorescent isothiocyanate; MFI, mean fluorescence intensity.

CONFLICT OF INTEREST

Y Urata is an employee of Oncolys BioPharma, Inc., the manufacturer of OBP-401 (Telomescan). The remaining authors declare no conflict of interest.

ACKNOWLEDGEMENTS

We thank Dr Satoru Kyo (Kanazawa University) for providing the OST cells; Dr Hiroyuki Kawashima (Niigata University) for providing the NOS-10 and NMFH-1 cells; and Tomoko Sueishi for her excellent technical support. This study was supported by grants-in-Aid from the Ministry of Education, Science and Culture, Japan and grants from the Ministry of Health and Welfare, Japan.

REFERENCES

1 Kanerva A, Hemminki A. Adenoviruses for treatment of cancer. *Ann Med* 2005; **37**: 33-43.
2 Rein DT, Breidenbach M, Curiel DT. Current developments in adenovirus-based cancer gene therapy. *Future Oncol* 2006; **2**: 137-143.
3 Yamamoto M, Curiel DT. Current issues and future directions of oncolytic adenoviruses. *Mol Ther* 2010; **18**: 243-250.
4 Clayman GL, el-Naggar AK, Lippman SM, Henderson YC, Frederick M, Merritt JA *et al.* Adenovirus-mediated p53 gene transfer in patients with advanced recurrent head and neck squamous cell carcinoma. *J Clin Oncol* 1998; **16**: 2221-2232.
5 Swisher SG, Roth JA, Nemunaitis J, Lawrence DD, Kemp BL, Carrasco CH *et al.* Adenovirus-mediated p53 gene transfer in advanced non-small-cell lung cancer. *J Natl Cancer Inst* 1999; **91**: 763-771.
6 Shimada H, Matsubara H, Shiratori T, Shimizu T, Miyazaki S, Okazumi S *et al.* Phase I/II adenoviral p53 gene therapy for chemoradiation resistant advanced esophageal squamous cell carcinoma. *Cancer Sci* 2006; **97**: 554-561.
7 Fujiwara T, Tanaka N, Kanazawa S, Ohtani S, Saijo Y, Nukiwa T *et al.* Multicenter phase I study of repeated intratumoral delivery of adenoviral p53 in patients with advanced non-small-cell lung cancer. *J Clin Oncol* 2006; **24**: 1689-1699.
8 Fujiwara T, Urata Y, Tanaka N. Telomerase-specific oncolytic virotherapy for human cancer with the hTERT promoter. *Curr Cancer Drug Targets* 2007; **7**: 191-201.
9 Pesonen S, Kangasniemi L, Hemminki A. Oncolytic adenoviruses for the treatment of human cancer: focus on translational and clinical data. *Mol Pharm* 2011; **8**: 12-28.
10 Bergelson JM, Cunningham JA, Droguett G, Kurt-Jones EA, Krithivas A, Hong JS *et al.* Isolation of a common receptor for Coxsackie B viruses and adenoviruses 2 and 5. *Science* 1997; **275**: 1320-1323.
11 Hemmi S, Geertsen R, Mezzacasa A, Peter I, Dummer R. The presence of human coxsackievirus and adenovirus receptor is associated with efficient adenovirus-mediated transgene expression in human melanoma cell cultures. *Hum Gene Ther* 1998; **9**: 2363-2373.
12 Hutchin ME, Pickles RJ, Yarbrough WG. Efficiency of adenovirus-mediated gene transfer to oropharyngeal epithelial cells correlates with cellular differentiation and human coxsackie and adenovirus receptor expression. *Hum Gene Ther* 2000; **11**: 2365-2375.
13 You Z, Fischer DC, Tong X, Hasenburg A, Aguilar-Cordova E, Kieback DG. Coxsackievirus-adenovirus receptor expression in ovarian cancer cell lines is associated with increased adenovirus transduction efficiency and transgene expression. *Cancer Gene Ther* 2001; **8**: 168-175.
14 Rauen KA, Sudilovsky D, Le JL, Chew KL, Hann B, Weinberg V *et al.* Expression of the coxsackie adenovirus receptor in normal prostate and in primary and metastatic prostate carcinoma: potential relevance to gene therapy. *Cancer Res* 2002; **62**: 3812-3818.
15 Kim M, Zinn KR, Barnett BG, Sumerel LA, Krasnykh V, Curiel DT *et al.* The therapeutic efficacy of adenoviral vectors for cancer gene therapy is limited by a low level of primary adenovirus receptors on tumour cells. *Eur J Cancer* 2002; **38**: 1917-1926.
16 Qin M, Chen S, Yu T, Escuadro B, Sharma S, Batra RK. Coxsackievirus adenovirus receptor expression predicts the efficiency of adenoviral gene transfer into non-small cell lung cancer xenografts. *Clin Cancer Res* 2003; **9**: 4992-4999.
17 Douglas JT, Kim M, Sumerel LA, Carey DE, Curiel DT. Efficient oncolysis by a replicating adenovirus (ad) *in vivo* is critically dependent on tumor expression of primary ad receptors. *Cancer Res* 2001; **61**: 813-817.
18 Fuxe J, Liu L, Malin S, Philipson L, Collins VP, Pettersson RF. Expression of the coxsackie and adenovirus receptor in human astrocytic tumors and xenografts. *Int J Cancer* 2003; **103**: 723-729.
19 Marsee DK, Vadysirisack DD, Morrison CD, Prasad ML, Eng C, Duh QY *et al.* Variable expression of coxsackie-adenovirus receptor in thyroid tumors: implications for adenoviral gene therapy. *Thyroid* 2005; **15**: 977-987.
20 Anders M, Rosch T, Kuster K, Becker I, Hofler H, Stein HJ *et al.* Expression and function of the coxsackie and adenovirus receptor in Barrett's esophagus and associated neoplasia. *Cancer Gene Ther* 2009; **16**: 508-515.
21 Korn WM, Macal M, Christian C, Lacher MD, McMillan A, Rauen KA *et al.* Expression of the coxsackievirus- and adenovirus receptor in gastrointestinal cancer correlates with tumor differentiation. *Cancer Gene Ther* 2006; **13**: 792-797.
22 Gu W, Ogose A, Kawashima H, Ito M, Ito T, Matsuba A *et al.* High-level expression of the coxsackievirus and adenovirus receptor messenger RNA in osteosarcoma, Ewing's sarcoma, and benign neurogenic tumors among musculoskeletal tumors. *Clin Cancer Res* 2004; **10**: 3831-3838.
23 Kawashima H, Ogose A, Yoshizawa T, Kuwano R, Hotta Y, Hotta T *et al.* Expression of the coxsackievirus and adenovirus receptor in musculoskeletal tumors and mesenchymal tissues: efficacy of adenoviral gene therapy for osteosarcoma. *Cancer Sci* 2003; **94**: 70-75.
24 Rice AM, Currier MA, Adams LC, Bharatan NS, Collins MH, Snyder JD *et al.* Ewing sarcoma family of tumors express adenovirus receptors and are susceptible to adenovirus-mediated oncolysis. *J Pediatr Hematol Oncol* 2002; **24**: 527-533.
25 Matsumoto K, Shariat SF, Ayala GE, Rauen KA, Lerner SP. Loss of coxsackie and adenovirus receptor expression is associated with features of aggressive bladder cancer. *Urology* 2005; **66**: 441-446.
26 Anders M, Vieth M, Rocken C, Ebert M, Pross M, Gretschel S *et al.* Loss of the coxsackie and adenovirus receptor contributes to gastric cancer progression. *Br J Cancer* 2009; **100**: 352-359.
27 Yamamoto S, Yoshida Y, Aoyagi M, Ohno K, Hirakawa K, Hamada H. Reduced transduction efficiency of adenoviral vectors expressing human p53 gene by repeated transduction into glioma cells *in vitro*. *Clin Cancer Res* 2002; **8**: 913-921.
28 Tango Y, Taki M, Shirakiya Y, Ohtani S, Tokunaga N, Tsunemitsu Y *et al.* Late resistance to adenoviral p53-mediated apoptosis caused by decreased expression of Coxsackie-adenovirus receptors in human lung cancer cells. *Cancer Sci* 2004; **95**: 459-463.
29 Sasaki T, Tazawa H, Hasei J, Kunisada T, Yoshida A, Hashimoto Y *et al.* Preclinical evaluation of telomerase-specific oncolytic virotherapy for human bone and soft tissue sarcomas. *Clin Cancer Res* 2011; **17**: 1828-1838.
30 Kawashima T, Kagawa S, Kobayashi N, Shirakiya Y, Umeoka T, Teraishi F *et al.* Telomerase-specific replication-selective virotherapy for human cancer. *Clin Cancer Res* 2004; **10** (1 Pt 1): 285-292.
31 Hashimoto Y, Watanabe Y, Shirakiya Y, Uno F, Kagawa S, Kawamura H *et al.* Establishment of biological and pharmacokinetic assays of telomerase-specific replication-selective adenovirus. *Cancer Sci* 2008; **99**: 385-390.
32 Kishimoto H, Kojima T, Watanabe Y, Kagawa S, Fujiwara T, Uno F *et al. In vivo* imaging of lymph node metastasis with telomerase-specific replication-selective adenovirus. *Nat Med* 2006; **12**: 1213-1219.
33 Kishimoto H, Urata Y, Tanaka N, Fujiwara T, Hoffman RM. Selective metastatic tumor labeling with green fluorescent protein and killing by systemic administration of telomerase-dependent adenoviruses. *Mol Cancer Ther* 2009; **8**: 3001-3008.
34 Kojima T, Hashimoto Y, Watanabe Y, Kagawa S, Uno F, Kuroda S *et al.* A simple biological imaging system for detecting viable human circulating tumor cells. *J Clin Invest* 2009; **119**: 3172-3181.
35 Kishimoto H, Zhao M, Hayashi K, Urata Y, Tanaka N, Fujiwara T *et al. In vivo* internal tumor illumination by telomerase-dependent adenoviral GFP for precise surgical navigation. *Proc Natl Acad Sci USA* 2009; **106**: 14514-14517.
36 Feero WG, Rosenblatt JD, Huard J, Watkins SC, Epperly M, Clemens PR *et al.* Viral gene delivery to skeletal muscle: insights on maturation-dependent loss of fiber infectivity for adenovirus and herpes simplex type 1 viral vectors. *Hum Gene Ther* 1997; **8**: 371-380.
37 Hoffman RM. The multiple uses of fluorescent proteins to visualize cancer *in vivo*. *Nat Rev Cancer* 2005; **5**: 796-806.
38 Hoffman RM, Yang M. Subcellular imaging in the live mouse. *Nat Protoc* 2006; **1**: 775-782.
39 Shay JW, Bacchetti S. A survey of telomerase activity in human cancer. *Eur J Cancer* 1997; **33**: 787-791.
40 Marsman WA, Buskens CJ, Wesseling JG, Offerhaus GJ, Bergman JJ, Tytgat GN *et al.* Gene therapy for esophageal carcinoma: the use of an explant model to test adenoviral vectors *ex vivo*. *Cancer Gene Ther* 2004; **11**: 289-296.
41 Wang Y, Thorne S, Hannock J, Francis J, Au T, Reid T *et al.* A novel assay to assess primary human cancer infectibility by replication-selective oncolytic adenoviruses. *Clin Cancer Res* 2005; **11**: 351-360.
42 Zeimet AG, Muller-Holzner E, Schuler A, Hartung G, Berger J, Hermann M *et al.* Determination of molecules regulating gene delivery using adenoviral vectors in ovarian carcinomas. *Gene Therapy* 2002; **9**: 1093-1100.
43 Kuster K, Koschel A, Rohwer N, Fischer A, Wiedenmann B, Anders M. Downregulation of the coxsackie and adenovirus receptor in cancer cells by hypoxia depends on HIF-1alpha. *Cancer Gene Ther* 2010; **17**: 141-146.

44 Seidman MA, Hogan SM, Wendland RL, Worgall S, Crystal RG, Leopold PL. Variation in adenovirus receptor expression and adenovirus vector-mediated transgene expression at defined stages of the cell cycle. *Mol Ther* 2001; **4**: 13-21.

45 Hotta T, Motoyama T, Watanabe H. Three human osteosarcoma cell lines exhibiting different phenotypic expressions. *Acta Pathol Jpn* 1992; **42**: 595-603.

46 Kawashima H, Ogose A, Gu W, Nishio J, Kudo N, Kondo N *et al.* Establishment and characterization of a novel myxofibrosarcoma cell line. *Cancer Genet Cytogenet* 2005; **161**: 28-35.

47 Kunisada T, Miyazaki M, Mihara K, Gao C, Kawai A, Inoue H *et al.* A new human chondrosarcoma cell line (OUMS-27) that maintains chondrocytic differentiation. *Int J Cancer* 1998; **77**: 854-859.

Supplementary Information accompanies the paper on Gene Therapy website (http://www.nature.com/gt)

European Journal of Cancer (2012) 48, 2282–2291

Available at www.sciencedirect.com

SciVerse ScienceDirect

journal homepage: www.ejconline.com

A novel apoptotic mechanism of genetically engineered adenovirus-mediated tumour-specific p53 overexpression through E1A-dependent p21 and MDM2 suppression

Yasumoto Yamasaki [a], Hiroshi Tazawa [a,b], Yuuri Hashimoto [a], Toru Kojima [a], Shinji Kuroda [a], Shuya Yano [a], Ryosuke Yoshida [a], Futoshi Uno [a], Hiroyuki Mizuguchi [c], Akira Ohtsuru [d], Yasuo Urata [e], Shunsuke Kagawa [a], Toshiyoshi Fujiwara [a,*]

[a] *Department of Gastroenterological Surgery, Okayama University Graduate School of Medicine, Dentistry and Pharmaceutical Sciences, Okayama 700-8558, Japan*
[b] *Center for Gene and Cell Therapy, Okayama University Hospital, Okayama 700-8558, Japan*
[c] *Department of Biochemistry and Molecular Biology, Graduate School of Pharmaceutical Sciences, Osaka University, Osaka 565-0871, Japan*
[d] *Takashi Nagai Memorial International Hibakusha Medical Center, Nagasaki University Hospital, Nagasaki 852-8501, Japan*
[e] *Oncolys BioPharma Inc., Tokyo 105-0001, Japan*

Available online 13 January 2012

KEYWORDS
Oncolytic adenovirus
Telomerase
p53
Apoptosis
p21

Abstract Oncolytic viruses engineered to replicate in tumour cells but not in normal cells could be used as tumour-specific vectors carrying the therapeutic genes. We previously developed a telomerase-specific oncolytic adenovirus, OBP-301, that causes cell death in human cancer cells with telomerase activities. Here, we further modified OBP-301 to express the wild-type *p53* tumour suppressor gene (OBP-702), and investigated whether OBP-702 induces stronger antitumour activity than OBP-301. The antitumour effect of OBP-702 was compared to that of OBP-301 on OBP-301-sensitive (H358 and H460) and OBP-301-resistant (T.Tn and HSC4) human cancer cells. OBP-702 suppressed the viability of both OBP-301-sensitive and OBP-301-resistant cancer cells more efficiently than OBP-301. OBP-702 caused increased apoptosis compared to OBP-301 or a replication-deficient adenovirus expressing the *p53* gene (Ad-p53) in H358 and T.Tn cells. Adenovirus E1A-mediated p21 and MDM2 downregulation was involved in the apoptosis caused by OBP-702. Moreover, OBP-702 significantly suppressed tumour growth in subcutaneous tumour xenograft models compared to monotherapy with OBP-301 or Ad-p53. Our data demonstrated that OBP-702 infection expressed adenovirus E1A and then inhibited p21 and MDM2 expression, which in turn efficiently induced apoptotic cell death. This novel apoptotic mechanism suggests that the p53-expressing OBP-702 is a promising antitumour reagent for human cancer and could improve the clinical outcome.

* *Corresponding author:* Address: Department of Gastroenterological Surgery, Okayama University Graduate School of Medicine, Dentistry and Pharmaceutical Sciences, 2-5-1 Shikata-cho, Kita-ku, Okayama 700-8558, Japan. Tel.: +81 86 235 7257; fax: +81 86 221 8775.
E-mail address: toshi_f@md.okayama-u.ac.jp (T. Fujiwara).

0959-8049/$ - see front matter © 2011 Elsevier Ltd. All rights reserved.
doi:10.1016/j.ejca.2011.12.020

1. Introduction

Replication-selective oncolytic viruses have emerged as promising antitumour reagents for induction of tumour-specific cell death.[1–4] Recent evidence from several clinical studies of oncolytic virotherapy has suggested that oncolytic viruses are well tolerated by cancer patients.[5–8] We previously developed a telomerase-specific replication-competent oncolytic adenovirus OBP-301 (Telomelysin), in which the human telomerase reverse transcriptase (*hTERT*) promoter drives the expression of the *E1A* and *E1B* genes that are linked to an internal ribosome entry site (IRES).[9–11] A phase I clinical trial of OBP-301 in patients with advanced solid tumours has been recently completed and OBP-301 was well tolerated by these patients.[12] However, the antitumour effect of OBP-301 was limited in some of the OBP-301-injected tumours. Therefore, to efficiently eliminate tumour cells using OBP-301, and to improve the clinical outcome of cancer patients, enhancement of the OBP-301-mediated antitumour effect is required.

Genetically engineered armed oncolytic viruses that express several types of therapeutic transgenes have recently been reported that were aimed at enhancing the antitumour effect of an oncolytic virus.[6,13] Among candidate therapeutic transgenes, the tumour-suppressor *p53* gene is a potent therapeutic transgene for induction of cell cycle arrest, senescence and apoptosis.[14] Indeed, a p53-expressing replication-deficient adenovirus (Ad-p53, Advexin) has been reported to induce an antitumour effect in both *in vitro* and *in vivo* settings[15,16] as well as in various clinical studies.[17–20] Recently, p53-expressing armed replication-selective oncolytic adenoviruses have been shown to induce a stronger antitumour effect than a non-armed oncolytic adenovirus or Ad-p53.[21–23] However, the molecular mechanism of the enhanced antitumour effect of a p53-armed oncolytic adenovirus remains unclear. We recently showed that, in combination therapy, OBP-301 enhanced Ad-p53-mediated apoptosis through p53 upregulation and by suppression of the p53-downstream target p21,[24] which is not only transcriptionally activated and mainly induces cell cycle arrest, but also suppresses apoptosis.[25] These results suggest that this p53-expressing oncolytic adenovirus has a strong antitumour effect through apoptosis induction.

In the present study, we first investigated whether the p53-expressing telomerase-specific replication-competent oncolytic adenovirus OBP-702 has efficient *in vitro* antitumour activity compared with OBP-301. We next compared the induction of apoptotic cell death of human cancer cells infected with OBP-301, OBP-702 and Ad-p53. The molecular mechanism of OBP-702-mediated apoptosis induction was further addressed. Finally, the *in vivo* antitumour effect of OBP-702 was evaluated using two subcutaneous human tumour xenograft models.

2. Materials and methods

2.1. Cell lines

The human non-small cell lung cancer cell lines H1299 (p53 null), H358 (p53 null) and H460 (wild-type p53) were obtained from the American Type Culture Collection (Manassas, VA, USA). The human oesophageal cancer cell line T.Tn (mutant-type p53) was purchased from the Japanese Collection Research Bioresources (JCRB, Osaka, Japan). The human oral squamous cell carcinoma cell line HSC4 (wild-type p53) was obtained from the Human Science Research Resources Bank (HSRRB, Osaka, Japan). The human colon cancer cell lines (SW620 (mutant-type p53) and LoVo (wild-type p53)) and the human liver cancer cell line HepG2 (wild-type p53) were obtained from the American Type Culture Collection (Manassas, VA, USA). The human liver cancer cell line Huh-7 (mutant-type p53) was obtained from the Human Science Research Resources Bank (HSRRB, Osaka, Japan). H1299, H358, H460, T.Tn, SW620 and LoVo cells were maintained in RPMI 1640 medium. HSC4, HepG2 and Huh-7 cells were maintained in Dulbecco's modified Eagle's medium. All media were supplemented with 10% foetal bovine serum, 100 U/ml penicillin and 100 mg/ml streptomycin. The cells were routinely maintained at 37 °C in a humidified atmosphere containing 5% CO_2.

2.2. Recombinant adenoviruses

The recombinant telomerase-specific, replication-competent adenovirus OBP-301 (Telomelysin), in which the promoter element of the *hTERT* gene drives the expression of *E1A* and *E1B* genes that are linked with an IRES, was previously constructed and characterised.[9–11] For OBP-301 induction of exogenous *p53* gene expression, a human wild-type *p53* gene expression cassette derived by the Egr-1 promoter was inserted into the E3 region of OBP-301 (Fig. 1A). The E1A-deleted adenoviral vector dl312 and the wild-type adenovirus type 5 (Ad5) were used as control vectors. Recombinant viruses were purified by ultracentrifugation using caesium chloride step gradients, their titres were determined by a plaque-forming assay using 293 cells, and viruses were stored at −80 °C.

2.3. Western blot analysis

Cells were seeded in a 100-mm dish at a density of 1×10^5 cells/dish 12 h before infection and were infected with OBP-301, OBP-702 or Ad-p53 at the indicated multiplicity of infection (MOI). Whole cell lysates were prepared in a lysis buffer (50 mM Tris–HCl (pH 7.4), 150 mM NaCl, 1% Triton X-100) containing a protease inhibitor cocktail (Complete Mini; Roche, Indianapolis,

IN, USA) at the indicated time points. Proteins were electrophoresed on 6–15% SDS polyacrylamide gels and were transferred to polyvinylidene difluoride membranes (Hybond-P; GE Healthcare, Buckinghamshire, UK). Blots were blocked with 5% non-fat dry milk in TBS-T (Tris-buffered saline and 0.1% Tween-20, pH 7.4) at room temperature for 30 min. The primary antibodies used were: mouse anti-p53 monoclonal antibody (mAb) (Calbiochem, Darmstadt, Germany), mouse anti-$p21^{WAF1}$ mAb (Calbiochem), mouse anti-MDM2 mAb (Santa Cruz Biotechnology, Santa Cruz, CA, USA), rabbit anti-BAX polyclonal antibody (pAb) (Santa Cruz Biotechnology), rabbit anti-poly (ADP-ribose) polymerase (PARP) pAb (Cell Signaling Technology, Beverly, MA, USA), mouse anti-Ad5 E1A mAb (BD PharMingen, Franklin Lakes, NJ, USA) and mouse anti-β-actin mAb (Sigma–Aldrich, St. Louis, MO, USA). The secondary antibodies used were: horseradish peroxidase-conjugated antibodies against rabbit IgG (GE Healthcare) or mouse IgG (GE Healthcare). Immunoreactive bands on the blots were visualised using enhanced chemiluminescence substrates (ECL Plus; GE Healthcare).

2.4. Cell viability assay

Cells were seeded on 96-well plates at a density of 1×10^3 cells/well 12 h before infection and were infected with OBP-301 or OBP-702 at MOIs of 0, 0.1, 1, 10 or 100 plaque-forming units (PFU)/cell. Cell viability was determined on days 2, 3 and 5 after virus infection using the Cell Proliferation Kit II (Roche Molecular Biochemicals, Indianapolis, IN, USA), which is based on an XTT, sodium 3′-[1-(phenylaminocarbonyl)-3,4-tetrazolium]-bis(4-methoxy-6-nitro)benzene sulphonic acid hydrate assay, according to the manufacturer's protocol. The 50% inhibiting dose (ID_{50}) value of OBP-301 and OBP-702 for each cell line was calculated using cell viability data obtained on day 5 after virus infection.

2.5. Flow cytometric analysis of active caspase-3 expression

Cells were incubated for 20 min on ice in Cytofix/Cytoperm solution (BD Biosciences, Franklin Lakes, NJ, USA), were labelled with phycoerythrin-conjugated rabbit anti-active caspase-3 mAb (BD Biosciences) for

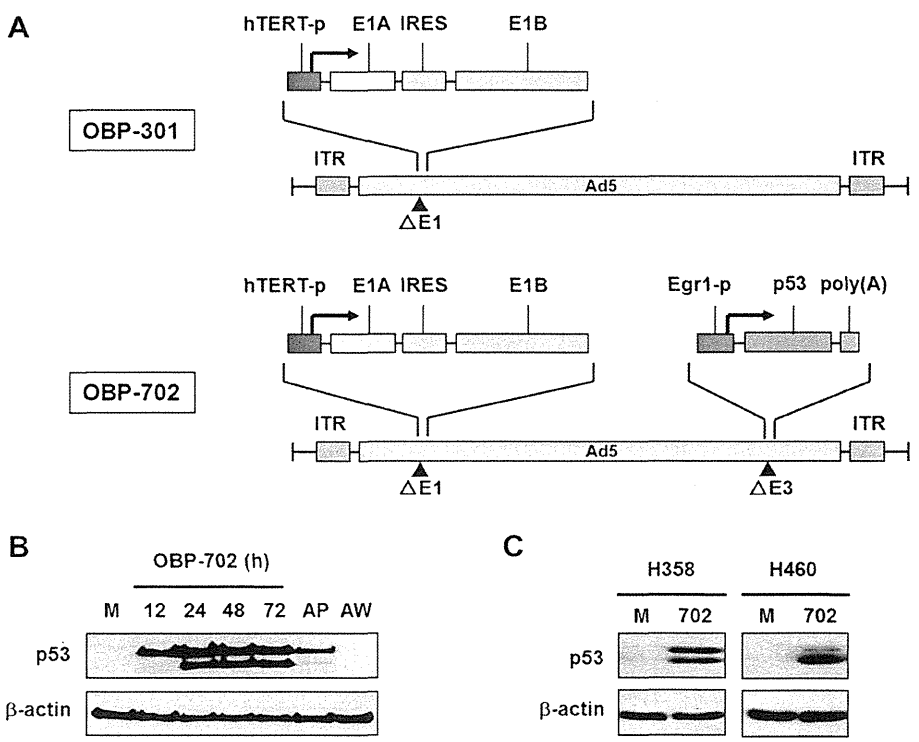

Fig. 1. p53 upregulation in human cancer cells infected with OBP-702. (A) Schematic diagrams of OBP-301 and OBP-702 structures. OBP-301 is a telomerase-specific replication-competent adenovirus, in which the *hTERT* promoter drives the expression of *E1A* and *E1B* genes that are linked with an IRES. OBP-702 is a p53-armed OBP-301, in which the *Egr-1* promoter drives expression of the *p53* gene that is inserted into the E3 region. (B) Expression of the p53 protein in p53-null H1299 cells infected with OBP-702 (10 MOI) at the indicated time points. A replication-deficient p53-expressing adenovirus Ad-p53 (AP) and a wild-type adenovirus Ad5 (AW) were also infected at an MOI of 10 for 24 h as a positive and negative control, respectively. Cell lysates were subjected to Western blot analysis with an anti-p53 antibody. β-Actin was assayed as a loading control. (C) Expression of the p53 protein in H358 and H460 cells infected with OBP-702 (702) at an MOI of 10 for 24 h. Mock-infected cells (M) were used as controls.

30 min, and were then analysed using FACS array (BD Biosciences).

2.6. In vivo subcutaneous H358 and T.Tn xenograft tumour models

Animal experimental protocols were approved by the Ethics Review Committee for Animal Experimentation of Okayama University School of Medicine. The H358 and T.Tn cells (5×10^6 cells per site) were inoculated into the flanks of 5-week-old female athymic nude mice (Charles River Laboratories, Wilmington, MA, USA). When tumours reached approximately 5–6 mm in diameter, a 50 μl volume of solution containing OBP-301, OBP-702 or Ad-p53 at a dose of 1×10^8 PFU or phosphate buffered saline (PBS) was injected into the tumours for three cycles every 2 days. Tumour size was monitored by measuring tumour length and width using calipers. Each tumour volume was calculated using the following formula: tumour volume (mm^3) = $L \times W^2 \times 0.5$, where L is the length and W is the width. The survival rate of mice with H358 tumours or T.Tn tumours was assessed until 90 or 180 days, respectively, after first treatment.

2.7. Statistical analysis

Data are expressed as means ± standard deviation (SD). Student's t test was used to compare differences between groups. Log-rank test was also used to compare differences between groups in the survival rate of mice. Statistical significance was defined as a P value less than 0.05.

3. Results

3.1. p53 induction in human cancer cells infected with OBP-702

To examine the level of p53 expression induced by OBP-702 in human cancer cells, we first evaluated p53 expression of p53-null human lung cancer H1299 cells after OBP-702 infection using Western blot analysis. The p53 expression level was increased within 24 h after OBP-702 infection, and a high expression level was maintained for up to 72 h (Fig. 1B). OBP-702-induced p53 expression was higher than Ad-p53-induced p53 expression 24 h after infection. Detectable 40 kDa protein expression in OBP-702-infected H1299 cells may be due to higher p53 expression. In contrast, no p53 expression was induced by OBP-301 infection (data not shown). OBP-702 further induced p53 expression in other human lung cancer cells (H358 (p53-null) and H460 (wild-type p53)) and in human colon cancer cells (SW620 (mutant p53), LoVo cells (wild-type p53)) and human liver cancer cells (HepG2 (wild-type p53) and Huh7 (mutant p53)) (Fig. 1C and Supplementary Fig. 1A). These results indicate that OBP-702 efficiently induces exogenous p53 expression in human cancer cells independent of the status of endogenous p53.

3.2. OBP-702 has enhanced antitumour activity against human cancer cells compared to OBP-301

To compare the *in vitro* antitumour activity of OBP-702 and OBP-301, we used the two OBP-301-sensitive human cancer cells (H358 and H460) and the two OBP-301-resistant human cancer cells (T.Tn and HSC4) that were previously reported.[11] OBP-301-resistant cells showed lower the coxsackie and adenovirus receptor (CAR) expression compared to OBP-301-sensitive cells (data not shown). The cell viability of each cell line was assessed over 5 days after infection using the XTT assay. OBP-702 suppressed the viability of OBP-301-sensitive and OBP-301-resistant cells more efficiently than OBP-301, although at least 48 h are required for the sufficient viral replication (Fig. 2A). Furthermore, OBP-702 also showed increased antitumour activity against human colon and liver cancer cells compared to OBP-301 (Supplementary Fig. 1B). Calculation of the ID_{50} values indicated that all cell lines were more sensitive to OBP-702 than to OBP-301 (Supplementary Table S1). These results suggest that OBP-702 is more cytopathic for human cancer cells than OBP-301.

3.3. Increased induction of apoptosis by OBP-702 compared to OBP-301 or Ad-p53

We next investigated whether OBP-702 has a greater apoptotic effect than OBP-301 or Ad-p53. OBP-301-sensitive H358 cells and OBP-301-resistant T.Tn cells were each infected with OBP-702, OBP-301 or Ad-p53 at MOIs of 10 and 100 for 48 h, and apoptosis was analysed. Western blot analysis showed that OBP-702, but not OBP-301 or Ad-p53, induced the cleavage of PARP at 48 and 72 h after infection (Fig. 3A). Furthermore, flow cytometric analysis demonstrated that OBP-702 infection significantly increased the percentage of apoptotic H358 and T.Tn cells that expressed active caspase-3 compared to Ad-p53 infection (Fig. 3B and C). However, no apoptosis was induced after OBP-301 infection. These results suggest that OBP-702 has a stronger effect on apoptosis than Ad-p53 or OBP-301.

3.4. Induction of apoptosis by OBP-702 through p53-dependent BAX upregulation and E1A-dependent p21 and MDM2 downregulation

Overexpression of p53 is well known to induce apoptosis through induction of p53-downstream target genes.[14] To investigate the molecular mechanism of OBP-702-induced apoptotic cell death, the expression

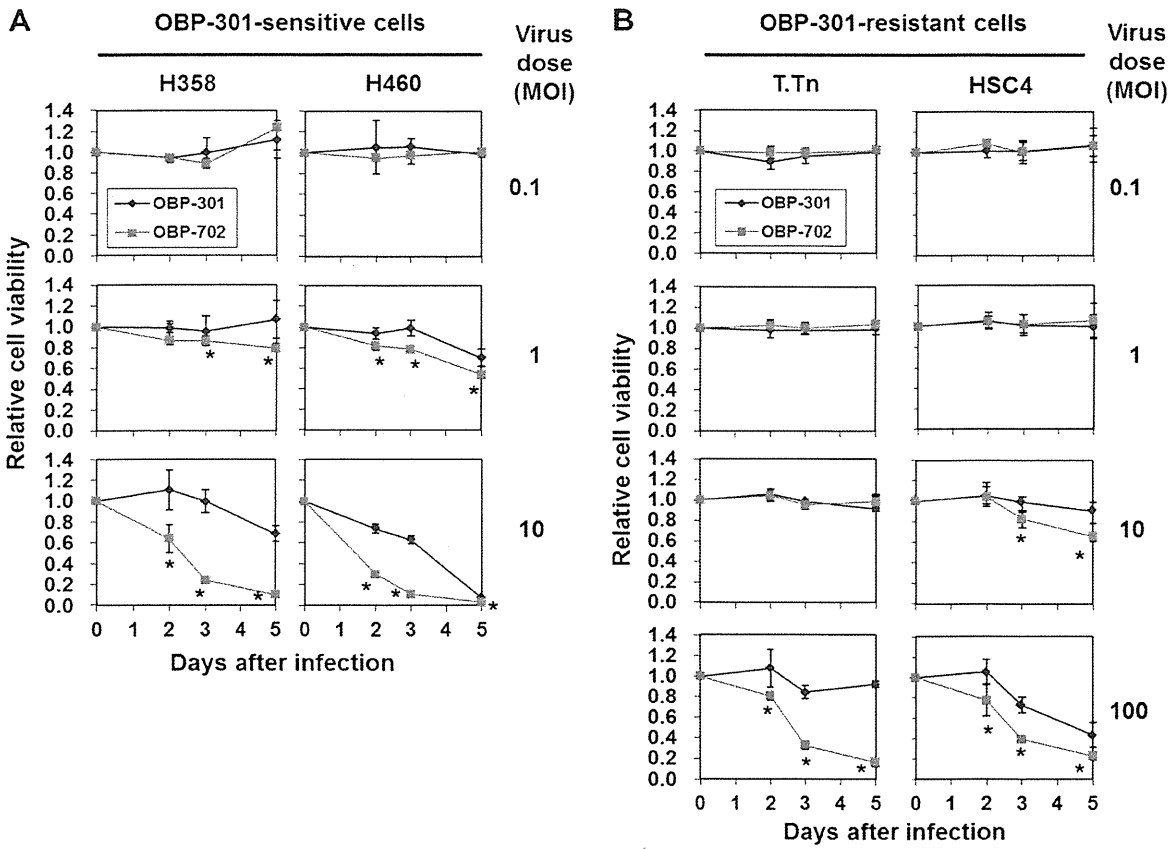

Fig. 2. OBP-702 has enhanced antitumour activity against human cancer cells compared to OBP-301. OBP-301-sensitive cells (H358 and H460) (A) and OBP-301-resistant cells (T.Tn and HSC4) (B) were infected with OBP-301 or OBP-702 at the indicated doses and cell viability was measured using the XTT assay on days 2, 3 and 5 after infection. Cell viability was calculated relative to that of the mock-treated group on each day, which was set at 1.0. Cell viability data are expressed as mean values ± SD ($n = 5$). Statistical significance was determined using Student's t test. $^{*}P < 0.05$. The data are representative of three separate experiments.

level of p53, and p53-downstream target proteins such as p21, BAX and MDM2, was evaluated by Western blot analysis. OBP-702 infection induced higher p53 expression than that induced by Ad-p53 between 24 and 72 h after infection (Fig. 4A). Ad-p53 infection upregulated the expression of p21, MDM2 and BAX proteins. In contrast, OBP-702 infection upregulated the BAX protein as well as Ad-p53, but expression of p21 and MDM2 was low despite strong p53 activation. PARP cleavage was observed 48 and 72 h after OBP-702 infection, consistent with suppression of p21 and MDM2 expression. Overexpression of the adenoviral E1A protein was observed in OBP-702-infected cells. These results suggest that OBP-702 upregulates p53 expression and subsequent BAX expression, but downregulates p21 and MDM2 expression, resulting in the induction of apoptosis.

We recently reported that OBP-301 enhances Ad-p53-induced apoptosis through p53 overexpression and p21 suppression.[24] Furthermore, adenovirus-mediated E2F1 overexpression also enhanced Ad-p53-induced apoptosis through MDM2 downregulation.[26] Since adenoviral E1A is known to activate E2F1 expression,[27] we hypothesised that OBP-702-mediated E1A expression may enhance Ad-p53-induced apoptosis through suppression of p21 and MDM2 expression. To address this hypothesis, H358 cells were coinfected with E1A-deficient dl312 or E1A-expressing wild-type Ad5 after Ad-p53 infection. Ad-p53-induced p53 overexpression was enhanced in the Ad5-coinfected H358 cells, but not in the dl312-coinfected H358 cells (Fig. 4B). Consistent with p53 overexpression, BAX expression was also upregulated. However, despite the enhanced p53 expression, the expression of p21 and MDM2 proteins was lower in Ad5-coinfected cells than in dl312-coinfected cells. Furthermore, PARP cleavage was only detected in H358 cells 72 h after coinfection of Ad-p53 with Ad5. As expected, OBP-301 infection had no apparent effect of the expression of p53, and p53-downstream target proteins (Supplementary Fig. 2). These results suggest that adenoviral E1A suppresses the expression of p21 and MDM2 thereby enhancing apoptosis through p53-dependent BAX upregulation (Fig. 4C, Supplementary Fig. 3).

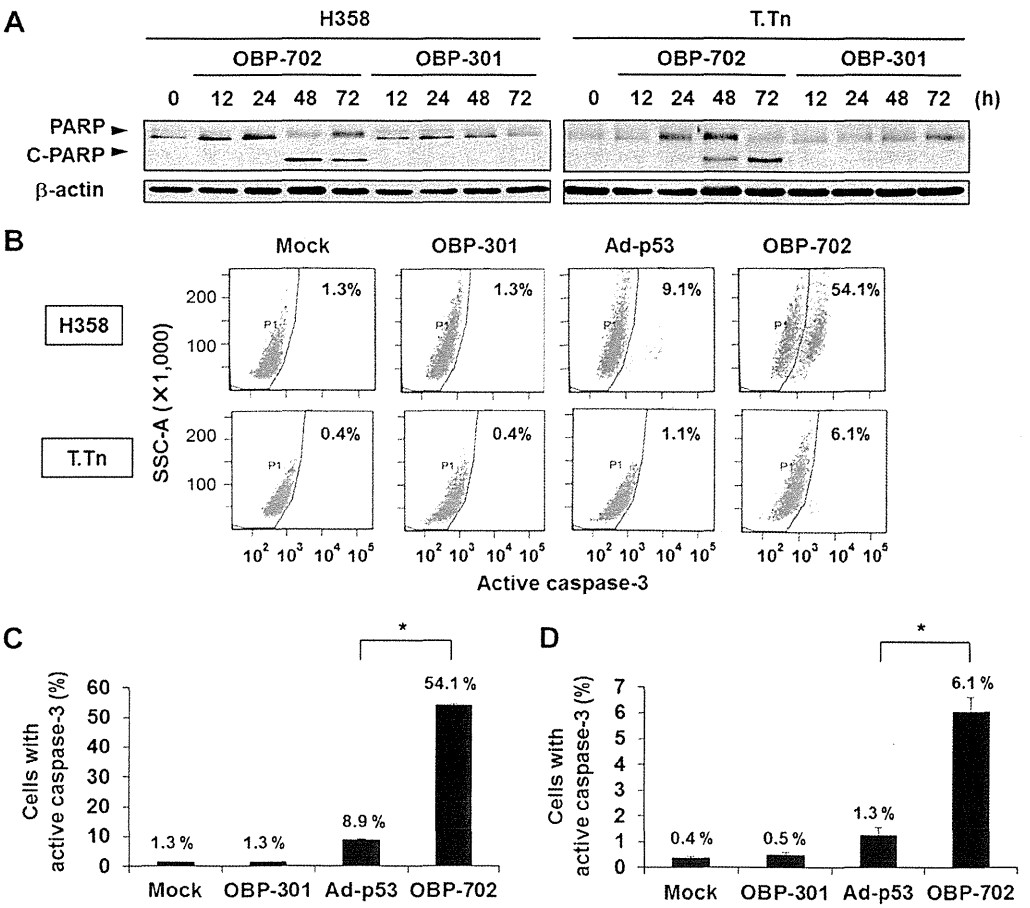

Fig. 3. OBP-702 induces increased apoptosis compared to OBP-301 or Ad-p53. (A) OBP-301-sensitive H358 cells and OBP-301-resistant T.Tn cells were infected with OBP-301 or OBP-702 at an MOI of 10 and 100, respectively, for 48 h. The level of cleaved PARP (C-PARP) and intact PARP in cell lysates was analysed using Western blotting. β-Actin was assayed as a loading control. (B–D), H358 and T.Tn cells were infected with OBP-702, OBP-301 or Ad-p53 at an MOI of 10 and 100, respectively, for 48 h. Mock-infected cells were used as controls. Caspase-3 activation was quantified using flow cytometric analysis. Representative flow cytometric data are shown (B). The mean percentage of H358 cells (C) and T.Tn cells (D) that express active caspase-3 was calculated based on three-independent experiments. Bars, SD. Statistical significance was determined using Student's *t* test. $^{*}P < 0.05$.

3.5. Enhanced antitumour effect of OBP-702 in tumour xenograft animal models

Finally, to assess the *in vivo* antitumour effect of OBP-702, we used subcutaneous H358 and T.Tn tumour xenograft models. OBP-702, OBP-301, Ad-p53 or PBS was intratumourally injected for three cycles every 2 days. OBP-702 administration significantly suppressed tumour growth compared to OBP-301, Ad-p53 or PBS in H358 and T.Tn tumour xenograft models (Fig. 5A). Furthermore, H358 tumour-bearing mice treated with OBP-702 significantly survived longer than those treated with OBP-301 or Ad-p53 (Fig. 5B). Although there was no significant difference in the survival rates between OBP-702-treated and OBP-301-treated mice with T.Tn tumours, OBP-702 treatment significantly increased the survival rate of T.Tn tumour-bearing mice compared to Ad-p53. These results suggest that OBP-702 eliminates tumour tissues more efficiently than OBP-301 or Ad-p53.

4. Discussion

Genetically engineered transgene-expressing armed oncolytic adenoviruses are expected to be a third-generation oncolytic virus for induction of a strong antitumour effect through induction of oncolytic and transgene-induced cell death.[6,13] Although the tumour suppressor *p53* gene is a potent therapeutic transgene for enhancement of an oncolytic adenovirus-mediated antitumour effect,[21–23] the molecular mechanisms by which p53 mediates enhancement of the antitumour effect remain unclear. In this study, we showed that the p53-expressing telomerase-specific oncolytic adenovirus OBP-702 exerted stronger *in vitro* and *in vivo* antitumour effects than OBP-301 or Ad-p53 (Figs. 2 and 5). This enhanced antitumour effect was due to p53-induced apoptosis, and adenoviral E1A enhanced this apoptosis via suppression of the expression of anti-apoptotic p21 and p53-inhibitory MDM2 (Figs. 3 and 4). Although

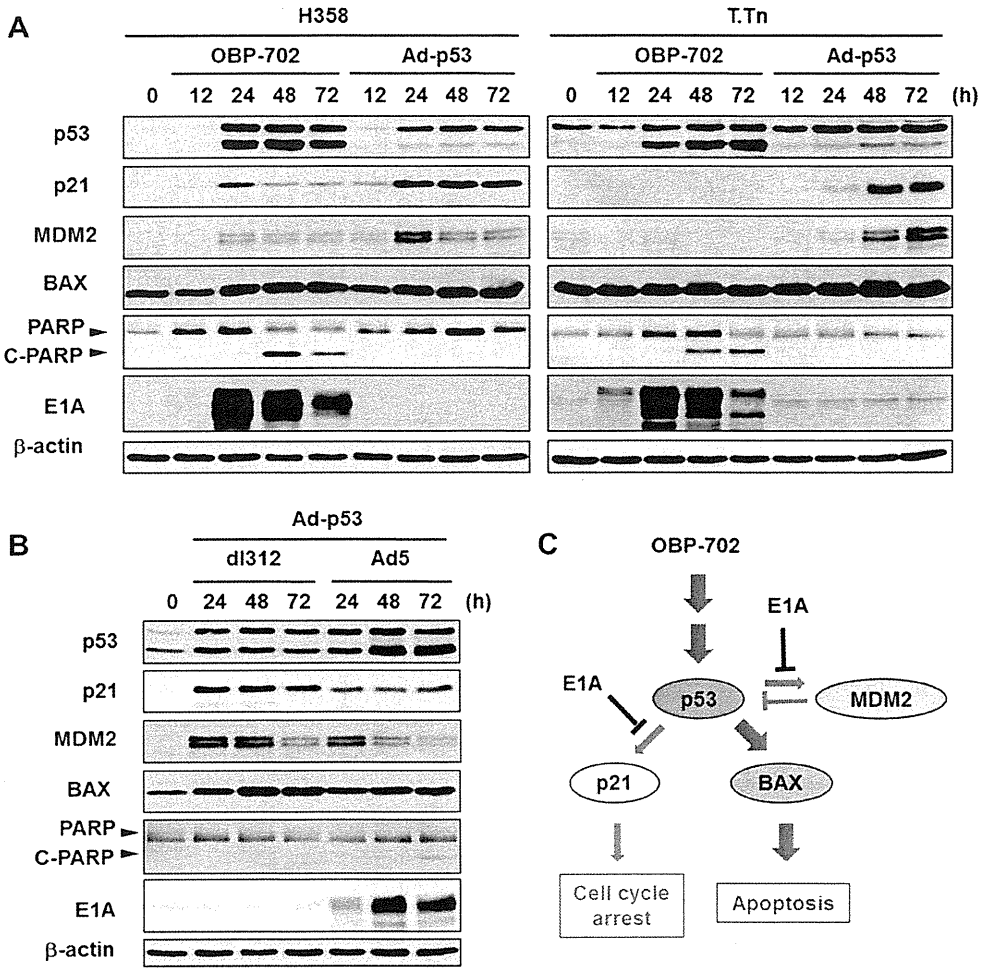

Fig. 4. OBP-702-mediated activation of p53, p53-target proteins and PARP in an E1A-dependent manner. (A) H358 and T.Tn cells were infected with OBP-702 or Ad-p53 at an MOI of 10 and 100, respectively, and infected cells were harvested at the indicated time points. The level of p53, p21, MDM2, BAX, PARP, cleaved PARP (C-PARP) and E1A proteins in cell lysates was analysed by Western blotting. β-Actin was assayed as a loading control. (B) H358 cells were infected with Ad-p53, following which they were coinfected with the E1A-deficient adenovirus (dl312) or an E1A-expressing wild-type adenovirus (Ad5) at the indicated time points. (C) Outline of OBP-702-mediated apoptosis induction through p53-dependent BAX upregulation and E1A-dependent downregulation of p21 and MDM2.

replication-competent adenovirus-mediated *p53* gene transduction has been suggested to exert an increased antitumour effect compared to replication-deficient Ad-p53 through replication-mediated p53 overexpression,[22] adenoviral E1A also enhanced p53-mediated apoptosis through suppression of expression of the p53-downstream targets p21 and MDM2 (Fig. 4). The adenoviral E1A protein has been previously shown to suppress p53-induced p21 and MDM2 expression.[28,29] E1A-mediated p21 and MDM2 suppression has also been shown to induce apoptosis in DNA-damaged cells that overexpress p53.[30,31] These reports support our findings that adenoviral E1A protein enhances p53-induced apoptosis through p21 and MDM2 suppression. It has recently been further shown that replication-deficient Ad-p53 enhances apoptosis through p21 suppression in combination with artificial microRNAs[32] or with OBP-301.[24] Thus, replication-competent oncolytic adenovirus-mediated *p53* gene transfer would strongly induce apoptosis not only through replication-dependent p53 overexpression, but also through E1A-dependent enhancement of p53-mediated apoptosis.

The molecular mechanism by which E1A suppresses p53-mediated upregulation of p21 and MDM2 remains unclear. Since adenoviral E1A has been shown to repress the expression of many target genes through activation of p300/CBP [cyclic adenosine monophosphate response element-binding protein (CREB)-binding protein] histone acetyltransferases that cause global histone modification,[33,34] p300/CBP activation may be involved in E1A-mediated p21 and MDM2 suppression. Indeed, E1A-mediated p21 and MDM2 suppression has been shown to be regulated in a p300/CBP dependent manner.[29,31] A recent report also suggested that an E1B-defective adenovirus activates p53 expression, but

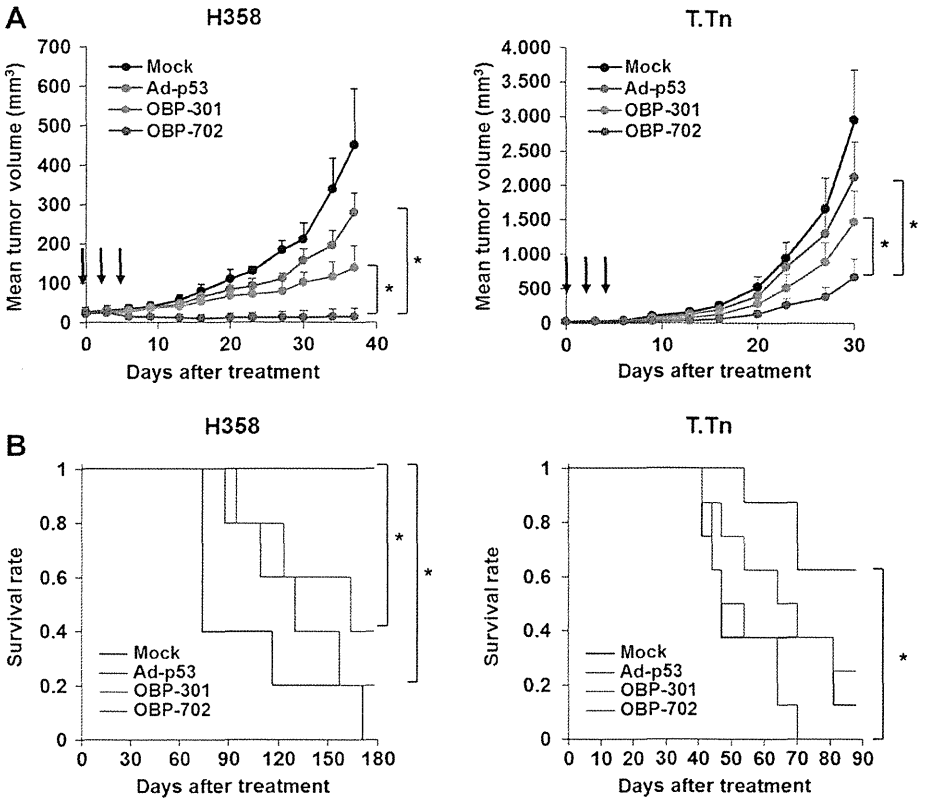

Fig. 5. Strong antitumour effect of OBP-702 on subcutaneous human tumours in xenograft models. (A) H358 or T.Tn cells (5×10^6 cells per site) were inoculated into the flank of 5-week-old female BALB/c *nu/nu* mice. When the tumours reached 3–5 mm in diameter, OBP-702 (10^8 PFU/tumour), OBP-301 (10^8 PFU/tumour), Ad-p53 (10^8 PFU/tumour) or PBS (Mock) was intratumourally injected on days 0, 2 and 4 (Black arrows). Tumour growth is expressed as the mean tumour volume ± SD in each group of H358 tumours ($n = 5$) or T.Tn tumours ($n = 8$). Statistical significance was determined using Student's *t* test. $^*P < 0.05$. The data are representative of three separate experiments. (B) Survival rate in each group of H358 tumours-bearing mice ($n = 5$) or T.Tn tumours-bearing mice ($n = 8$) was shown using the Kaplan–Meier method. Statistical significance was determined using log-rank test. $^*P < 0.05$.

suppresses p21 and MDM2 expression, through the binding of E1A with p300/CBP.[35] However, p300 disruption has also been shown to both increase p53 stability through MDM2 suppression, and to suppress p21 expression, resulting in apoptosis in UV-irradiated human cancer cells.[36] Therefore, the role of p300/CBP in adenoviral E1A-mediated p21 and MDM2 suppression may be cell type-specific.

It has recently been shown that siRNA-mediated p21 suppression enhances the antitumour effect of an oncolytic adenovirus,[37,38] suggesting that p21 suppression further induces oncolytic cell death. Oncolytic adenovirus-mediated cell death has been shown to be associated with autophagy-related cell death, which is distinct from apoptosis.[39,40] Autophagy has been shown to be positively regulated by p53,[14] but negatively regulated by p21.[41] These results suggest that p53 upregulation without p21 activation enhances autophagic cell death. Thus, oncolytic adenovirus-mediated p21 suppression may enhance not only p53-mediated apoptosis, but also autophagic cell death during the OBP-702-mediated antitumour effect.

Telomerase-specific replication-competent OBP-301 that possesses the *hTERT* gene promoter replicates, and induces an antitumour effect in, human cancer cells in a telomerase-dependent manner.[9–11] Previous reports have shown that Ad-p53-mediated p53 overexpression suppresses *hTERT* mRNA expression,[42,43] suggesting possible suppression of OBP-301 and OBP-702 replication by p53 overexpression. However, we previously reported that Ad-p53-mediated p53 overexpression did not suppress OBP-301 replication during combination therapy.[24] Shats et al. previously reported that knockdown of p21 eliminated the p53-dependent repression of *hTERT* mRNA expression.[44] Since OBP-702, or combination therapy of OBP-301 with Ad-p53, induces p53 overexpression together with E1A-mediated p21 downregulation, p53 overexpression may not suppress hTERT expression. Furthermore, we recently demonstrated that OBP-301 infection itself induces a 1.1- to 50-fold increase in *hTERT* mRNA expression in an E1A-dependent manner.[45] Thus, OBP-702-mediated p53 overexpression would induce apoptosis without affecting hTERT expression.

An anti-tumour effect of Ad-p53-mediated gene therapy has been shown in various clinical studies.[17–20] We previously reported that Ad-p53 induces sensitivity to chemotherapeutic drugs, resulting in enhancement of the antitumour effect.[46,47] Since OBP-702-mediated p53 gene transfer has a stronger antitumour effect than Ad-p53 (Fig. 5), combination therapy of OBP-702 with chemotherapeutic agents may be a more effective antitumour therapy than monotherapy of OBP-702. The adenoviral E1A protein has been shown to enhance chemotherapy-induced apoptosis.[48,49] In particular, p21 suppression has been suggested to be involved in E1A-mediated chemosensitisation.[30] Indeed, artificial miRNA-mediated p21 suppression on Ad-p53-induced p53 overexpression enhanced tumour sensitivity to chemotherapeutic agents.[32] Thus, combination therapy of a p53-armed oncolytic adenovirus with chemotherapy may be a more efficient antitumour strategy for eradication of tumour cells through p53 and E1A-mediated chemosensitisation than monotherapy.

In conclusion, we have clearly demonstrated that the p53-expressing oncolytic adenovirus OBP-702 has a much stronger antitumour effect than OBP-301 or Ad-p53 through p53-mediated apoptosis that is enhanced by E1A-dependent p21 and MDM2 suppression. Oncolytic adenovirus-mediated *p53* gene transduction should therefore be a promising antitumour therapy for efficient elimination of tumour cells.

Conflict of interest statement

Yasuo Urata is an employee of Oncolys BioPharma Inc., the manufacturer of OBP-301 (Telomelysin). Other authors declare no potential conflict of interest.

Acknowledgements

We thank Ms. Tomoko Sueishi and Mitsuko Yokota for their excellent technical support. This study was supported by grants from the Japan Science and Technology Agency (T.F. and H.T.); by grants from the Ministry of Health, Labour, and Welfare of Japan (T.F.) and by grants from the Ministry of Education, Culture, Sports, Science and Technology, Japan (H.T.).

Appendix A. Supplementary data

Supplementary data associated with this article can be found, in the online version, at doi:10.1016/j.ejca.2011.12.020.

References

1. Kirn D, Martuza RL, Zwiebel J. Replication-selective virotherapy for cancer: biological principles, risk management and future directions. *Nat Med* 2001;7(7):781–7.
2. Hawkins LK, Lemoine NR, Kirn D. Oncolytic biotherapy: a novel therapeutic platform. *Lancet Oncol* 2002;**3**(1):17–26.
3. Chiocca EA. Oncolytic viruses. *Nat Rev Cancer* 2002;**2**(12):938–50.
4. Vaha-Koskela MJ, Heikkila JE, Hinkkanen AE. Oncolytic viruses in cancer therapy. *Cancer Lett* 2007;**254**(2):178–216.
5. Aghi M, Martuza RL. Oncolytic viral therapies – the clinical experience. *Oncogene* 2005;**24**(52):7802–16.
6. Liu TC, Galanis E, Kirn D. Clinical trial results with oncolytic virotherapy: a century of promise, a decade of progress. *Nat Clin Pract Oncol* 2007;**4**(2):101–17.
7. Pesonen S, Kangasniemi L, Hemminki A. Oncolytic adenoviruses for the treatment of human cancer: focus on translational and clinical data. *Mol Pharm* 2011;**8**(1):12–28.
8. Eager RM, Nemunaitis J. Clinical development directions in oncolytic viral therapy. *Cancer Gene Ther* 2011;**18**(5):305–17.
9. Kawashima T, Kagawa S, Kobayashi N, et al. Telomerase-specific replication-selective virotherapy for human cancer. *Clin Cancer Res* 2004;**10**(1 Pt. 1):285–92.
10. Fujiwara T, Urata Y, Tanaka N. Telomerase-specific oncolytic virotherapy for human cancer with the hTERT promoter. *Curr Cancer Drug Targets* 2007;**7**(2):191–201.
11. Hashimoto Y, Watanabe Y, Shirakiya Y, et al. Establishment of biological and pharmacokinetic assays of telomerase-specific replication-selective adenovirus. *Cancer Sci* 2008;**99**(2):385–90.
12. Nemunaitis J, Tong AW, Nemunaitis M, et al. A phase I study of telomerase-specific replication competent oncolytic adenovirus (Telomelysin) for various solid tumors. *Mol Ther* 2010;**18**(2):429–34.
13. Cody JJ, Douglas JT. Armed replicating adenoviruses for cancer virotherapy. *Cancer Gene Ther* 2009;**16**(6):473–88.
14. Vousden KH, Prives C. Blinded by the light: the growing complexity of p53. *Cell* 2009;**137**(3):413–31.
15. Blagosklonny MV, el-Deiry WS. In vitro evaluation of a p53-expressing adenovirus as an anti-cancer drug. *Int J Cancer* 1996;**67**(3):386–92.
16. Zeng Y, Prabhu N, Meng R, Eldeiry W. Adenovirus-mediated p53 gene therapy in nasopharyngeal cancer. *Int J Oncol* 1997;**11**(2):221–6.
17. Clayman GL, el-Naggar AK, Lippman SM, et al. Adenovirus-mediated p53 gene transfer in patients with advanced recurrent head and neck squamous cell carcinoma. *J Clin Oncol* 1998;**16**(6):2221–32.
18. Swisher SG, Roth JA, Nemunaitis J, et al. Adenovirus-mediated p53 gene transfer in advanced non-small-cell lung cancer. *J Natl Cancer Inst* 1999;**91**(9):763–71.
19. Shimada H, Matsubara H, Shiratori T, et al. Phase I/II adenoviral p53 gene therapy for chemoradiation resistant advanced esophageal squamous cell carcinoma. *Cancer Sci* 2006;**97**(6):554–61.
20. Fujiwara T, Tanaka N, Kanazawa S, et al. Multicenter phase I study of repeated intratumoral delivery of adenoviral p53 in patients with advanced non-small-cell lung cancer. *J Clin Oncol* 2006;**24**(11):1689–99.
21. van Beusechem VW, van den Doel PB, Grill J, Pinedo HM, Gerritsen WR. Conditionally replicative adenovirus expressing p53 exhibits enhanced oncolytic potency. *Cancer Res* 2002;**62**(21):6165–71.
22. Zhao HC, Zhang Q, Yang Y, et al. P53-expressing conditionally replicative adenovirus CNHK500-p53 against hepatocellular carcinoma in vitro. *World J Gastroenterol* 2007;**13**(5):683–91.
23. Wang X, Su C, Cao H, et al. A novel triple-regulated oncolytic adenovirus carrying p53 gene exerts potent antitumor efficacy on common human solid cancers. *Mol Cancer Ther* 2008;7(6):1598–603.
24. Sakai R, Kagawa S, Yamasaki Y, et al. Preclinical evaluation of differentially targeting dual virotherapy for human solid cancer. *Mol Cancer Ther* 2010;**9**(6):1884–93.

25. Gorospe M, Cirielli C, Wang X, et al. P21(Waf1/Cip1) protects against p53-mediated apoptosis of human melanoma cells. *Oncogene* 1997;**14**(8):929–35.
26. Itoshima T, Fujiwara T, Waku T, et al. Induction of apoptosis in human esophageal cancer cells by sequential transfer of the wild-type p53 and E2F-1 genes: involvement of p53 accumulation via ARF-mediated MDM2 down-regulation. *Clin Cancer Res* 2000;**6**(7):2851–9.
27. Bagchi S, Raychaudhuri P, Nevins JR. Adenovirus E1A proteins can dissociate heteromeric complexes involving the E2F transcription factor: a novel mechanism for E1A trans-activation. *Cell* 1990;**62**(4):659–69.
28. Steegenga WT, van Laar T, Riteco N, et al. Adenovirus E1A proteins inhibit activation of transcription by p53. *Mol Cell Biol* 1996;**16**(5):2101–9.
29. Somasundaram K, El-Deiry WS. Inhibition of p53-mediated transactivation and cell cycle arrest by E1A through its p300/CBP-interacting region. *Oncogene* 1997;**14**(9):1047–57.
30. Chattopadhyay D, Ghosh MK, Mal A, Harter ML. Inactivation of p21 by E1A leads to the induction of apoptosis in DNA-damaged cells. *J Virol* 2001;**75**(20):9844–56.
31. Thomas A, White E. Suppression of the p300-dependent mdm2 negative-feedback loop induces the p53 apoptotic function. *Genes Dev* 1998;**12**(13):1975–85.
32. Idogawa M, Sasaki Y, Suzuki H, et al. A single recombinant adenovirus expressing p53 and p21-targeting artificial microRNAs efficiently induces apoptosis in human cancer cells. *Clin Cancer Res* 2009;**15**(11):3725–32.
33. Horwitz GA, Zhang K, McBrian MA, et al. Adenovirus small e1a alters global patterns of histone modification. *Science* 2008;**321**(5892):1084–5.
34. Ferrari R, Pellegrini M, Horwitz GA, et al. Epigenetic reprogramming by adenovirus e1a. *Science* 2008;**321**(5892):1086–8.
35. Savelyeva I, Dobbelstein M. Infection with E1B-mutant adenovirus stabilizes p53 but blocks p53 acetylation and activity through E1A. *Oncogene* 2011;**30**(7):865–75.
36. Iyer NG, Chin SF, Ozdag H, et al. P300 regulates p53-dependent apoptosis after DNA damage in colorectal cancer cells by modulation of PUMA/p21 levels. *Proc Natl Acad Sci USA* 2004;**101**(19):7386–91.
37. Shiina M, Lacher MD, Christian C, Korn WM. RNA interference-mediated knockdown of p21(WAF1) enhances anti-tumor cell activity of oncolytic adenoviruses. *Cancer Gene Ther* 2009;**16**(11):810–9.
38. Hoti N, Chowdhury WH, Mustafa S, et al. Armoring CRAds with p21/Waf-1 shRNAs: the next generation of oncolytic adenoviruses. *Cancer Gene Ther* 2010;**17**(8):585–97.
39. Ito H, Aoki H, Kuhnel F, et al. Autophagic cell death of malignant glioma cells induced by a conditionally replicating adenovirus. *J Natl Cancer Inst* 2006;**98**(9):625–36.
40. Jiang H, Gomez-Manzano C, Aoki H, et al. Examination of the therapeutic potential of Delta-24-RGD in brain tumor stem cells: role of autophagic cell death. *J Natl Cancer Inst* 2007;**99**(18):1410–4.
41. Fujiwara K, Daido S, Yamamoto A, et al. Pivotal role of the cyclin-dependent kinase inhibitor p21WAF1/CIP1 in apoptosis and autophagy. *J Biol Chem* 2008;**283**(1):388–97.
42. Kusumoto M, Ogawa T, Mizumoto K, et al. Adenovirus-mediated p53 gene transduction inhibits telomerase activity independent of its effects on cell cycle arrest and apoptosis in human pancreatic cancer cells. *Clin Cancer Res* 1999;**5**(8):2140–7.
43. Kanaya T, Kyo S, Hamada K, et al. Adenoviral expression of p53 represses telomerase activity through down-regulation of human telomerase reverse transcriptase transcription. *Clin Cancer Res* 2000;**6**(4):1239–47.
44. Shats I, Milyavsky M, Tang X, et al. P53-dependent down-regulation of telomerase is mediated by p21wafl. *J Biol Chem* 2004;**279**(49):50976–85.
45. Sasaki T, Tazawa H, Hasei J, et al. Preclinical evaluation of telomerase-specific oncolytic virotherapy for human bone and soft tissue sarcomas. *Clin Cancer Res* 2011;**17**(7):1828–38.
46. Fujiwara T, Grimm EA, Mukhopadhyay T, et al. Induction of chemosensitivity in human lung cancer cells in vivo by adenovirus-mediated transfer of the wild-type p53 gene. *Cancer Res* 1994;**54**(9):2287–91.
47. Ogawa N, Fujiwara T, Kagawa S, et al. Novel combination therapy for human colon cancer with adenovirus-mediated wild-type p53 gene transfer and DNA-damaging chemotherapeutic agent. *Int J Cancer* 1997;**73**(3):367–70.
48. Cook JL, Routes BA, Walker TA, Colvin KL, Routes JM. E1A oncogene induction of cellular susceptibility to killing by cytolytic lymphocytes through target cell sensitization to apoptotic injury. *Exp Cell Res* 1999;**251**(2):414–23.
49. Cook JL, Miura TA, Ikle DN, Lewis Jr AM, Routes JM. E1A oncogene-induced sensitization of human tumor cells to innate immune defenses and chemotherapy-induced apoptosis in vitro and in vivo. *Cancer Res* 2003;**63**(12):3435–43.

uicc
global cancer control

IJC
International Journal of Cancer

Genetically engineered oncolytic adenovirus induces autophagic cell death through an E2F1-*microRNA-7*-epidermal growth factor receptor axis

Hiroshi Tazawa[1,2], Shuya Yano[2], Ryosuke Yoshida[2], Yasumoto Yamasaki[2], Tsuyoshi Sasaki[3], Yuuri Hashimoto[2], Shinji Kuroda[2], Masaaki Ouchi[4], Teppei Onishi[2], Futoshi Uno[2], Shunsuke Kagawa[2], Yasuo Urata[4] and Toshiyoshi Fujiwara[2]

[1] Center for Gene and Cell Therapy, Okayama University Hospital, Okayama, Japan
[2] Department of Gastroenterological Surgery, Okayama University Graduate School of Medicine, Dentistry and Pharmaceutical Sciences, Okayama, Japan
[3] Department of Orthopaedic Surgery, Okayama University Graduate School of Medicine, Dentistry and Pharmaceutical Sciences, Okayama, Japan
[4] Oncolys BioPharma Inc., Tokyo, Japan

Autophagy is known to have a cytoprotective role under various cellular stresses; however, it also results in robust cell death as an important safeguard mechanism that protects the organism against invading pathogens and unwanted cancer cells. Autophagy is regulated by cell signalling including microRNA (miRNA), a post-transcriptional regulator of gene expression. Here, we show that genetically engineered telomerase-specific oncolytic adenovirus induced *miR-7* expression, which is significantly associated with its cytopathic activity in human cancer cells. Virus-mediated *miR-7* upregulation depended on enhanced expression of the E2F1 protein. Ectopic expression of *miR-7* suppressed cell viability and induced autophagy by inhibiting epidermal growth factor receptor (EGFR) expression. Our results suggest that oncolytic adenovirus induces autophagic cell death through an E2F1-*miR-7*-EGFR pathway in human cancer cells, providing a novel insight into the molecular mechanism of an anticancer virotherapy.

Autophagy is well known to have a cytoprotective role and to contribute to the maintenance of cell survival under various cellular stresses, such as deprivation of nutrients,[1] hypoxia[2] and interruption of growth signaling.[3] The autophagic process has also been associated with the inhibition of tumor development. In fact, it has been reported that adenovirus infection induces autophagy-related cell death in infected cancer cells, leading to tumor suppression.[4–6] Furthermore, oncolytic adenoviruses induce autophagic cell death in human malignant glioma cells[7,8] and in brain tumor stem cells.[9] However, the molecular mechanism underlying virus infection-mediated autophagic cell death remains unclear.

MicroRNA (miRNA) is a small noncoding RNA consisting of 22 nucleotides, which post-transcriptionally suppresses the expression of many target genes by pairing with complementary nucleotide sequences in the 3′-untranslated regions of the target mRNA. A number of reports have indicated that miRNA can regulate diverse cell fates including cell proliferation,[10] the epithelial-mesenchymal transition,[11] apoptosis[12] and senescence[13] in cancer cells. Recently, Zhu *et al.* demonstrated inhibition of autophagy by *miR-30a*, which suppresses the autophagy-related *beclin 1* gene in human cancer cells,[14] suggesting the possible regulation of autophagy in cancer cells by miRNA. In addition, the Epstein-Barr virus[15] and the human cytomegalovirus[16] have been reported to modulate cellular miRNA expression in normal infected cells. The adenoviral E1A protein also downregulated *miR-520h* expression, resulting in an antitumor effect.[17]

These observations led us to examine whether genetically engineered telomerase-specific oncolytic adenovirus modulate cellular miRNA expression in human cancer cells. We previously developed an oncolytic adenovirus, OBP-301, which drives the expression of viral *E1A* and *E1B* genes linked with an internal ribosome entry site under the control of the

Key words: adenovirus, telomerase, microRNA, autophagy, EGFR
Abbreviations:: Ad5: wild-type adenovirus serotype 5; AVO: acidic vesicular organelle; CAR: coxsackie and adenovirus receptor; EGFR: epidermal growth factor receptor; GFP: green fluorescent protein; hTERT: human telomerase reverse transcriptase; LC3: microtubule-associated protein 1 light chain 3; 3-MA: 3-methyladenine; miRNA: microRNA; MOI: multiplicity of infection; PFU: plaque-forming units; RT-PCR: reverse transcription-polymerase chain reaction
Additional Supporting Information may be found in the online version of this article.
Grant sponsors: Japan Science and Technology Agency, Ministry of Health, Labour, and Welfare of Japan, Ministry of Education, Culture, Sports, Science and Technology, Japan
DOI: 10.1002/ijc.27589
History: Received 5 Aug 2011; Accepted 13 Mar 2012; Online 11 Apr 2012
Correspondence to: Toshiyoshi Fujiwara, Department of Gastroenterological Surgery, Okayama University Graduate School of Medicine, Dentistry and Pharmaceutical Sciences, 2-5-1 Shikata-cho, Kita-ku, Okayama 700-8558, Japan, Tel.: +81-86-235-7257, Fax: +81-86-221-8775, E-mail: toshi_f@md.okayama-u.ac.jp

human telomerase reverse transcriptase (*hTERT*) promoter for virus replication and, therefore, induces oncolytic cell death in human cancer cells with high telomerase activity, but not in human normal cells without telomerase activity.[18] OBP-301 has an antitumor effect against a variety of human cancer cells in both *in vitro* and *in vivo* settings.[18,19] In this study, we investigated whether OBP-301- and wild-type adenovirus-mediated cytopathic activities are associated with autophagy induction in human cancer and normal cells. To address the molecular mechanism on the oncolytic adenovirus-induced autophagy, we assessed the global miRNA modulation in the infected cells and identified the miRNA-based autophagy induction system during adenovirus infection.

Material and Methods

Cell lines

The human nonsmall cell lung cancer cell lines H1299 and A549 were obtained from the American Type Culture Collection (Manassas, VA). The human esophageal cancer cell line T.Tn was purchased from Japanese Collection Research Bioresources (Osaka, Japan). The human normal lung fibroblast cell line NHLF was obtained from TaKaRa Biomedicals (Kyoto, Japan). The H1299 and T.Tn cells were maintained in RPMI 1640 medium, and A549 cells were maintained in Dulbecco's modified Eagle's medium containing a Nutrient Mixture (Ham's F-12). All media were supplemented with 10% fetal bovine serum, 100 U/ml penicillin and 100 mg/ml streptomycin. NHLF cells were cultured in the medium recommended by the manufacturer. The cells were routinely maintained at 37°C in a humidified atmosphere with 5% CO_2.

Recombinant adenovirus

Construction and characterization of the recombinant tumor-specific replication-selective adenovirus vector OBP-301 (Telomelysin) was previously reported.[18,19] Ad5 was the basal adenovirus for OBP-301 and was also used as another type of replication-competent adenovirus. Replication-deficient adenoviral vectors expressing E2F1 (Ad-E2F1) were used to induce E2F1 expression in infected cells, as previously reported.[20] OBP-301, Ad5 and Ad-E2F1 were purified using CsCl step gradient ultracentrifugation followed by CsCl linear gradient ultracentrifugation.

Infection of cells with OBP-301 or Ad5 and cell viability assay

Cells were seeded on 96-well plates at a density of 1×10^3 cells/well 12 hr before infection and were infected with OBP-301 or Ad5 at MOIs of 0, 1, 5, 10, 50 and 100 plaque-forming units/cell. Cell viability was determined on day 3 after infection using the Cell Proliferation Kit II (Roche Molecular Biochemicals, Indianapolis, IN) according to the manufacturer's protocol.

Transfection of cells with siRNA or miRNA and cell viability assay

Cells seeded at a density of 5×10^2 cells/well in 96-well plates were transfected with either p62 siRNA (Applied Biosystems, Foster City, CA) or with control siRNA (Applied Biosystems) at a concentration of 0, 1, 5 or 10 nM using HiPerfect transfection reagents (Qiagen, Valencia, CA). *miR-7* (Ambion, Austin, TX) or control miRNA (Ambion) was also transfected at the same concentrations. In contrast, EGFR siRNA (Applied Biosystems) or control siRNA (Applied Biosystems) was treated at a concentration of 0, 10 and 50 nM. Cells were pretreated with 3-methyladenine (3-MA) (200 nM) (Sigma–Aldrich, St. Louis, MO) for 2 hr before transfection to inhibit *miR-7*-mediated autophagy. Cell viability was determined on day 6 after transfection using the Cell Proliferation Kit II (Roche Molecular Biochemicals).

Western blot analysis

Cells were seeded in a 100-mm dish at a density of 1×10^5 cells/dish 12 hr before transfection and were transfected with either *miR-7* (Ambion) or with control miRNA (Ambion) at a concentration of 10 nM, or were infected with OBP-301 at the indicated MOIs. On day 3 after treatment, whole cell lysates were prepared in a lysis buffer (50 mM Tris–HCl (pH 7.4), 150 mM NaCl and 1% Triton X-100) containing a protease inhibitor cocktail (Complete Mini; Roche). Proteins were electrophoresed on 6–15% SDS polyacrylamide gels and were transferred to polyvinylidene difluoride membranes (Hybond-P; GE Health Care, Buckinghamshire, UK). Blots were blocked with 5% nonfat dry milk in TBS-T (Tris-buffered saline and 0.1% Tween-20, pH 7.4) at room temperature for 30 min. The primary antibodies used were: rabbit antimicrotubule-associated protein 1 light chain 3 (LC3) polyclonal antibody (pAb) (Medical & Biological Laboratories (MBL), Nagoya, Japan), rabbit anti-Atg5 pAb (Cosmo Bio, Tokyo, Japan), mouse anti-p62 monoclonal antibody (mAb) (MBL), mouse anti-Ad5 E1A mAb (BD PharMingen, Franklin Lakes, NJ), rabbit anti-E2F1 pAb (Santa Cruz Biotechnology, Santa Cruz, CA), goat anti-wild-type EGFR pAb (R&D Systems Inc., Minneapolis, MN) and mouse anti-β-actin mAb (Sigma-Aldrich). The secondary antibodies used were: horseradish peroxidase-conjugated antibodies against rabbit IgG (GE Healthcare), mouse IgG (GE Healthcare) or goat IgG (Chemicon International Inc., Temecula, CA). Immunoreactive bands on the blots were visualized using enhanced chemiluminescence substrates (ECL Plus; GE Healthcare).

Quantitative real-time reverse transcription-PCR analysis

Cells were seeded on six-well plates at a density of 3×10^4 cells/well 12 hr before infection and were infected with either OBP-301 or with Ad5 at the indicated MOIs. Total RNA was extracted from cells using a miRNeasy Mini kit (Qiagen).

Total RNA was extracted in dose-dependent experiments from cells infected at the indicated MOIs on day 3 after infection, and in time-course experiments from cells on days 0, 1, 2, 3 and 4 after infection. cDNA was synthesized from 10 ng of total RNA using the TaqMan MicroRNA Reverse Transcription kit (Applied Biosystems), and quantitative real-time RT-PCR was performed using the Applied Biosystems StepOnePlus™ real-time PCR system. The expression of *miR-7* was defined from the threshold cycle (Ct), and relative expression levels were calculated using the $2^{-\Delta\Delta Ct}$ method after normalization with reference to the expression of U6 snRNA.

miRNA microarray

The cells were seeded in 75T flasks at a density of 2.0×10^5 cells/flask 12 hr before infection and were infected with either OBP-301 or Ad5 using an MOI of 5. Total RNA, including miRNA, was extracted from the OBP-301-infected, Ad5-infected and mock-infected cells on day 3 after infection using a miRNeasy Mini kit (Qiagen) according to the manufacturer's protocol, and RNA concentrations were quantified using a NanoDrop spectrophotometer. The RNA samples were then used for microarray analysis, which was performed by Exiqon (Vedbaek, Denmark) (http://www.exiqon.com/). For this analysis, each RNA sample and a mixture of all samples were labeled with Hy3 or Hy5, respectively, and were hybridized with three dual-color miRNA microarray chips (miRCURY™ LNA Array version 10.0; Exiqon) in which 719 kinds of human miRNA probes were contained. Fifteen miRNAs showed more than a 50% difference in expression between the OBP-301- or Ad5-infected cells and the mock-infected cells (Supporting Information Fig. 4a). The expression levels of *miR-33a*, *miR-183*, *miR-483-3p* and *miR-7* were evaluated using real-time RT-PCR, as described above.

Infection of cells with E2F1-expressing adenoviral vectors and treatment with E2F1 siRNA

H1299 and A549 cells, seeded at a density of 3×10^4 cells/well in six-well plates, were infected with Ad-E2F1 at an MOI of 100 for 2 days. The same cell lines, seeded at the same density in six-well plates, were transfected with E2F1 siRNA (Applied Biosystems) or control siRNA (Applied Biosystems) at a concentration of 10 nM and, 24 hr later, were infected with 5 or 50 MOI (H1299 and A549 cells, respectively) of OBP-301 for 3 days. Total RNA and whole cell lysates were prepared from the infected cells, and the expression levels of *miR-7* and E2F1 were analyzed using real-time RT-PCR and western blotting, respectively.

Determination of autophagic cells using H1299-GFP-LC3 cells

H1299 cells stably transfected with GFP and LC3 fusion plasmid (GFP-LC3) were previously established.[9] After transfection with 50 nM *miR-7* (Ambion) or control miRNA (Ambion), GFP expression in the transfected cells was examined using a laser confocal microscope (Fluoview 300; Olympus, Tokyo, Japan). As a positive control, H1299-GFP-LC3 cells were serum-starved by culture in Hank's balanced salt solution for 4 hr before laser confocal microscopy (Olympus).

Flow cytometry

A549 cells, seeded at a density of 1×10^5 cells/dish in 100-mm dishes, were transfected with either 10 nM *miR-7* (Ambion) or control miRNA (Ambion) for 3 days. Following staining with Acridine Orange solution (1.0 μg/ml; Sigma–Aldrich) for 15 min, the cells were trypsinized and were analyzed using a flow cytometer (FACSArray; Becton Dickinson, San Jose, CA).

Statistical analysis

Determination of significant differences was assessed using Student's *t*-test. Correlations between the expression levels of *miR-7*, the cytopathic activity of OBP-301 and the expression level of EGFR were analyzed using Pearson's correlation coefficient. $p < 0.05$ was considered significant.

Results

The cytopathic effect of the oncolytic adenovirus OBP-301 is associated with induction of autophagy in human cancer cells

To investigate if the cytopathic effect of OBP-301 correlates with autophagy in human cancer cells, we used three human cancer cell lines (H1299, A549 and T.Tn), that showed different sensitivities to OBP-301.[19,21] The cytopathic effect of OBP-301 against each cell line was determined by assay of cell viability using the XTT assay (Fig. 1*a*). The H1299 and A549 cells showed high and moderate sensitivities, respectively, to OBP-301, but T.Tn cells were resistant. T.Tn cells showed lower expression level of coxsackie and adenovirus receptor (CAR) protein, but similar *hTERT* mRNA expression compared to H1299 and A549 cells (Supporting Information Figs. 1a and 2a). Consistent with CAR expression, T.Tn cells were less sensitive to adenovirus-mediated green fluorescent protein (GFP) induction compared to H1299 and A549 cells (Supporting Information Fig. 1b). In spite of high hTERT expression, the replication rate of OBP-301 was suppressed in T.Tn cells compared to H1299 and A549 cells (Supporting Information Fig. 2b). These results suggest that its resistance was due to impairment of virus infection and replication. Furthermore, as OBP-301 shows the tumor-specific cytopathic effect in a telomerase-dependent manner, the cell viability of human normal fibroblasts (NHLF), which show low CAR expression and no *hTERT* mRNA expression (Supporting Information Figs. 1a and 2a), was also determined after infection with OBP-301. As reported previously,[18] NHLF cells showed the resistance to OBP-301-mediated cytopathic effect (Fig. 1*a*). The cytopathic activity and replication rate of wild-type adenovirus serotype 5 (Ad5)

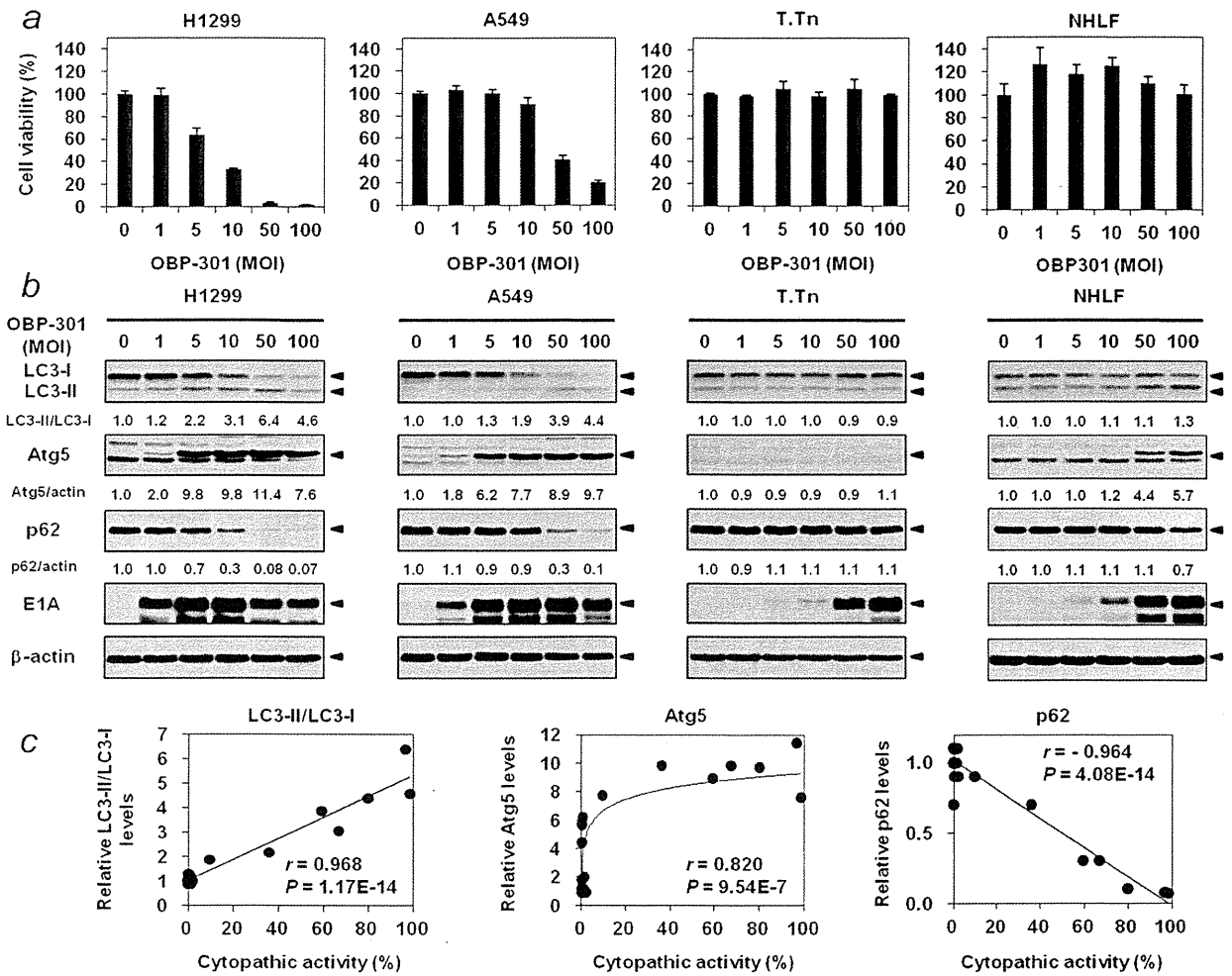

Figure 1. OBP-301-mediated induction of autophagic cell death in human cancer cells. (*a*) The cytopathic effect of OBP-301 in human cancer cells (H1299, A549 and T.Tn) and normal fibroblasts (NHLF). Cell viability was determined 72 hr after infection with OBP-301 at the indicated MOIs, using an XTT assay. Cell viability was calculated relative to that of mock infected cells, whose viability was set at 100%. (*b*) Expression of the autophagy marker proteins microtubule-associated protein 1 light chain 3 (LC3), Atg5, p62 and the viral E1A protein in H1299, A549, T.Tn and NHLF cells infected with OBP-301 at the indicated MOIs for 72 hr was assessed using Western blotting. β-actin was assayed as a loading control. The expression level of each protein was calculated relative to its expression in mock-infected cells, whose expression level was designated as 1. (*c*) There was a significant correlation between the expression levels of autophagy marker proteins (LC3-II, Atg5 and p62) and the cytopathic activity of OBP-301.

were also confirmed in all cell lines (Supporting Information Figs. 2 and 3). The data for the sensitivities to OBP-301 and Ad5 and expression levels of CAR and hTERT were summarized in Supporting Information Table 1.

Oncolytic adenovirus-mediated autophagy can be characterized by conversion of the microtubule-associated protein 1 light chain 3 (LC3)-I to the LC3-II form,[7,22,23] by upregulation of the autophagy-related protein Atg5[9,23] and by downregulation of the p62 protein.[23] Therefore, to analyze OBP-301 induction of autophagy, we determined the expression levels of LC3-I/II, Atg5 and p62 proteins in OBP-301-infected cells by Western blot analysis (Fig. 1*b*). OBP-301-sensitive H1299 and A549 cells exhibited conversion of LC3-I to LC3-II, Atg5 upregulation and p62 downregulation after OBP-301 infection using more than five multiplicity of infections (MOIs). However, the OBP-301-resistant T.Tn cells and NHLF cells showed no induction of autophagy. Adenoviral E1A expression was detected in all four cell lines after infection with OBP-301. To further evaluate the relationship between OBP-301-induced autophagy and cytopathic effect, OBP-301-sensitive cells were infected with OBP-301 at an MOI of 50, and the morphological and autophagic changes were analyzed at 0, 24, 48 and 72 hr after infection using conventional microscopy, Western blot analysis and electron microscopy (Supporting Information Figs. 3 and 4). Although no morphological and autophagic changes were observed at